IDENTIFICATION AND CHARACTERIZATION OF A NADPH OXIDASE TARGET IN *FUSARIUM GRAMINEARUM*

by

Salima Chatur

A thesis submitted to the Faculty of Graduate and Postdoctoral Affairs in partial fulfillment of the requirements for the degree of

Master of Science

in

Biology

Carleton University
Ottawa, Ontario

Abstract

Fusarium graminearum is a fungal plant pathogen that causes Fusarium Head Blight (FHB) on important food and feed cereal crops including wheat, maize and barley. Earlier studies identified distinct roles for NADPH oxidase (NOX) genes in *F. graminearum.* NOX enzymes generate reactive oxygen species (ROS) including hydrogen peroxide (H_2O_2), which are important in signal transduction. To elucidate the mechanism of NOX dependent signaling in pathogenicity, a proteomics approach was used to examine redox changes in the *ΔnoxA/B* mutant and compared to wildtype *F. graminearum* strain. Candidate substrates of NOX enzymes were characterized by genetic analysis. Deletion and overexpression of one of the candidate genes, *FGSG_10089* with modified cysteine residues confirmed that it is likely a genuine substrate of the NOX enzyme complex. Bioinformatics and expression analysis indicate that this protein may function as a virulence factor. Deletion of *FGSG_10089* as well as modification of the cysteine residue C^{325} resulted in reduced virulence on wheat. In addition, there was a decrease in production of 15-acetyl deoxynivalenol in culture.

Acknowledgements

I would like to thank my supervisor Dr. Gopal Subramaniam for his guidance and patience in helping me develop my research and writing skills. His enthusiasm for scientific progress and innovation is infectious and inspiring. Furthermore, I am grateful to my co-supervisor Owen Rowland and committee members Dr. Willmore and Dr. Vierula for their insights and assistance.

I would also like to acknowledge the scientists, technicians and students at Agriculture Canada who provided their advice and expertise through the course of this project including Sean Walkowiak and Chris Bonner for general and bioinformatics advice, Denise Chabot for the confocal microscopy, Anne Herman for Western blot assistance, and Li Wang and Chris Mogg for technical assistance.

Table of Contents

List of Figures

List of Tables

List of Abbreviations

2-DE - Two-Dimensional Gel Electrophoresis

3-ADON - 3-acetyldeoxynivalenol

15-ADON - 15-acetyldeoxynivalenol

CMC - Carboxymethyl cellulose

CFW - Calcofluor white

CWDE - Cell wall degrading enzymes

DON - Deoxynivalenol

FHB - Fusarium Head Blight

GPI - Glycosylphosphatidylinositol

GSH - Glutathione

GTP - Guanosine triphosphate

LC-MS/MS - Liquid Chromatography-Tandem Mass Spectrometry

MAPK - Mitogen activated protein kinase

MW - Molecular weight

NADPH - Nicotinamide adenine dinucleotide phosphate

NCBI - National centre for biotechnology

NIV - Nivalenol

NOX - NADPH oxidase

qRT-PCR - Quantitative real time polymerase chain reaction

QTL - Quantitative trait loci

ROS - Reactive oxygen species

YPD - Yeast peptone dextrose

Chapter 1 Literature review

1.1 *Fusarium Head Blight*- An overview

Canada is known for the amount and quality of wheat (*Triticum aestivum)* it produces. In 2012, the production was about 27 million tonnes, which places Canada as the 7th largest wheat producing nation in the world (Alberta wheat commission, 2013). One of the most prevalent biotic threats to this production level in North America is the pathogen *Fusarium graminearum* (Trail, 2009*)*. *F. graminearum* is the primary fungal species in Canada that causes blight on cereal crops (Goswami & Kistler, 2004). This filamentous ascomycete causes a reduction in yield through bleached and shriveled grain with dark lesions. Collectively, such symptoms are referred to as FHB- Fusarium Head Blight. Since the early 1990s, Canadian losses have ranged from $50 million to $300 million annually (Alberta agriculture, 2012). Furthermore, accumulation of mycotoxins produced by the pathogen such as deoxynivalenol (DON) and its derivatives in the infected wheat heads renders the crop unsafe for human consumption (Kazan *et al*., 2012). Following consumption, acute effects include nausea, vomiting and convulsions. Chronic symptoms include neurological effects and compromised immunity in humans (Goswami & Kistler, 2004). As a result, global regulations are in place to limit the toxin levels in grain by the European Union and the United States. Health Canada has also set limits and guidelines for the presence of DON at 1mg/kg (2011, CFIA). From an economic perspective, an export commodity that does not meet these stringent guidelines contributes to financial loss. These limitations place an increasing pressure to understand the mechanism behind *Fusarium* virulence.

1.2 Life cycle of *Fusarium graminearum*

F. graminearum is a hemi-biotrophic fungus, meaning that it has two distinct phases during the infection process. The disease cycle (Figure 1) begins with the infection of wheat florets when they are most susceptible, which is usually during spring time when conditions are conducive for *Fusarium* germination (high humidity). Crop debris, after the harvest stage, is the primary source of inoculum since perithecia are able to survive saprophytically during the winter (Brown *et al*., 2000; Kazan *et al*., 2012). Perithecia are fruiting bodies that are dark black, flask-shaped structures, which hold the tubular sacs called asci that discharge the sexual spores called ascospores (Bai, 2004). The ascospores that are released enter through natural openings at the base of the lemma and palea of the spikelet or through degenerating anther tissues (Trail, 2009) (Figure 2). In this early or the biotrophic phase, once a floret has been infected, the initial phase of intercellular growth on the glume is asymptomatic suggesting that during this phase the pathogen does not depend on host nutrient sources.

Previously, *Fusarium* had been described not to form specialized fungal structures, such as appressorium, for penetration (Bushnell *et al*., 2003). But recent microscopic examinations show that short bulbous infection structures occur early in the infection stage (Boenisch *et al*., 2011). These structures, which are referred to as infection cushions, can appear as lobed, thickened, and as branched hyphae and are associated with the expression of *Tri5,* which encodes for trichodiene synthase, the initial enzyme involved in the synthesis of the trichothecene DON (Boenisch *et al.*, 2011). Evidence also suggests that initial infection structures and lesions form independently of trichothecene production (Jansen *et al*., 2005). Thus, it is hypothesized that there are other virulence

factors secreted by the fungi which are involved in the initial infection stages that have yet to be discovered**.**

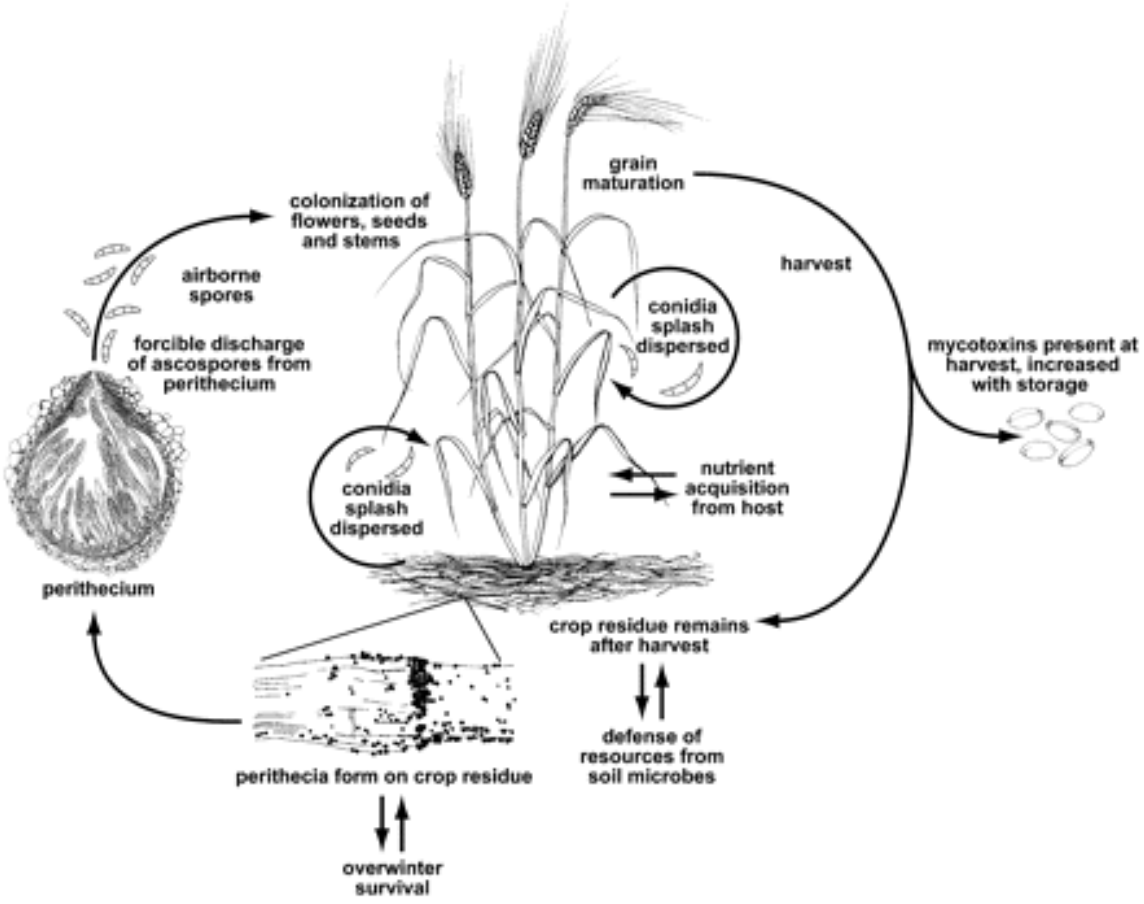

Figure 1: Life cycle of *Fusarium graminearum* as it infects wheat. Trail F. Plant Physiol. 2009:149:103-110. Copyright © 2009. American Society of Plant Biologists. All rights reserved.

During the second phase or the necrotrophic phase of the infection process, there is degeneration of host tissue, resulting in the release of nutrients. It is proposed that during this phase of infection, expression and secretion of cell wall degrading enzymes (CWDE) including cellulases, xylanases, pectinases and lipases occur (Kang *et al*., 2005; Rampitsch *et al*., 2013). Among the secreted proteins are included several glycosylphosphatidylinositol (GPI) -anchor proteins, which play an essential role in fungal cell wall remodeling to support mycelia growth at the infection front (Phalip *et al*., 2005). This process results in the penetration of growing hyphae into the ovary and floral brackets, which leads to further cellular degradation in the glume (Figure 2) (Pritsch *et al*., 2000; Brown *et al*., 2010). This intracellular growth through the vascular tissue allows for acquisition of nutrients from the plant and leads to a large amount of tissue necrosis. Symptoms start to appear as water soaked brown spots and leads to bleaching, as blockage of the vasculature become predominant (Trail, 2009). At the end of this cycle, hyphal structures called sporodochia produce septate conidia on the wheat heads. These asexual spores called macroconidia are responsible for short distance spread between the crop plants (Deacon, 2006).

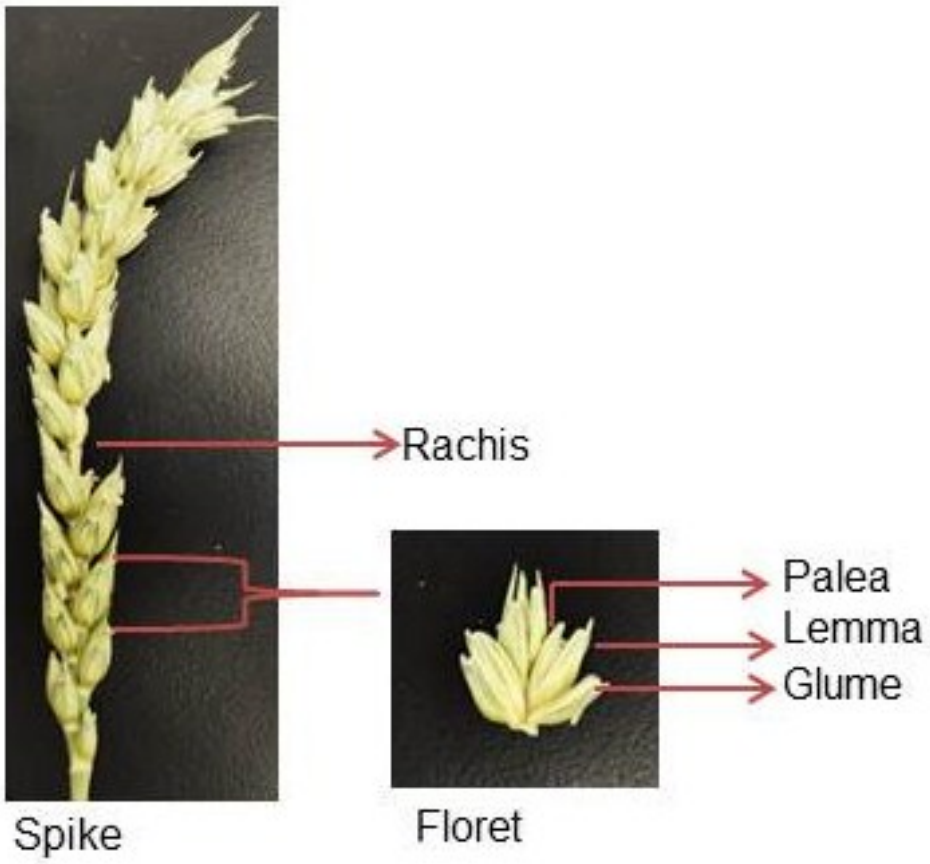

Figure 2: A depiction of the anatomy of a wheat spike and floret

1.3 Control of FHB- Resistance mechanisms in wheat

Fungicides such as tebuconazole have been used to control *Fusarium* and reduce DON in wheat; however, it is not always successful. Consistency in application is difficult, since anthesis varies within the field, and additionally, strains can also develop resistance (Wegulo *et al*., 2015). Other than chemical application, traditional breeding has historically been used to control FHB. Two major forms of resistance mechanisms have been characterized in wheat. Type I resistance, which is a resistance to initial infection and Type II resistance, associated with the spread of infection. An example of type II resistance is thickening of the cell walls at the rachis node to obstruct spread (Jansen *et al*., 2005). Other types of resistance have also been described including type III resistance, which is resistance to kernel infection, type IV resistance occurs when there is tolerance to trichothecenes and FHB, and type V, which is resistance to the accumulation of toxin (Miller *et al*., 1984; Mesterházy, 1995).

Many years of research have indicated that resistance to *Fusarium* is quantitative. Quantitative trait loci (QTL) analyses have identified several loci associated with FHB resistance (Gunnaiah *et al*., 2012). However, genes contributing to FHB resistance have not been identified. Evidence from several metabolome studies found increased presence of secondary metabolites such as hydroxycinnamic acid amides (HCAAs), which strengthen the cell wall at the rachis to increase resistance (Gunnaiah *et al*., 2012; Buerstmayr *et al*., 2009). One of the drawbacks with the breeding programs is that experimental wheat lines that show increased resistance to FHB, tend to not have good agronomic or quality traits (Kushalappa *et al*., 2010). Moreover, breeding for strong

resistance has not been particularly effective, especially in areas or conditions where FHB epidemics occur.

1.4 Pathogenicity factors contribute to *Fusarium* virulence

F. graminearum is a broad range pathogen that causes diseases on many cereal crops (Goswami and Kistler, 2004). This suggests that this pathogen has the ability to adapt to different host environments. Therefore, it has been proposed that *Fusarium* might encode a large number (up to 10% of the genome) of pathogenicity or virulence factors to infect its hosts (Ma *et al*., 2013). These factors could include phytotoxic secondary metabolites; gene products that disengage enzymes produced by hosts (e.g. proteases and chitinases) or suppress host defence (Paper *et al*., 2007; Rampitsch *et al*., 2013). In this regard, very few proteins encoded by *F. gramineraum* have been described as genuine virulence factors. However, the availability of genome sequences of many *Fusarium* species will accelerate identification of many more of these factors. The following sections will describe factors that have been identified as being necessary for the development of FHB on wheat.

1.4.1 Secondary metabolites as virulence factors

Genome sequences of several isolates of *F. graminearum* indicated that it is comprised of four chromosomes with an average genome size of 36.1 Mb (Trail, 2009; Cuomo *et al*., 2007). It is estimated to encode 13,937 predicted proteins. Analysis of the *F. graminearum* genome sequence identified 16 polyketide synthases, 19 non-ribosomal peptide synthases and 8 terpene synthases. This is remarkable because previous analyses have shown that this is equivalent to the genetic potential of the entire genus (Ma *et al*.,

2013). These enzymes catalyze condensation or rearrangement of structurally simple molecules to form more complex structures: non ribosomal peptides, polyketides, or terpenes. These chemical products typically undergo multiple enzymatic modifications to form biologically active secondary metabolites. In *Fusarium* and many other fungi, genes of a particular secondary metabolite biosynthetic pathway are usually physically clustered. In addition to the enzymes that utilize and tailor the parent compounds, secondary metabolite biosynthetic gene clusters also encode transporters that move the metabolites across membranes and pathway-specific transcription factors that activate expression of genes in a cluster (Ma *et al*., 2013).

One secondary metabolite that is synthesized by a cluster of enzymes and regulators is the trichothecene mycotoxin produced by *F. graminearum.* It is a sesquiterpene epoxide that has a 12, 13-epoxy-trichothe-9-ene structure (Figure 3), which can be chemically modified with functional groups at various positions to produce four types of toxins (Figure 3). Biologically active compounds that are derived from the *Tri* gene cluster include nivalenol which is the result of C-4 oxygenation; calonectrin is produced by *Tri1*, which hydroxylates carbon 7, and 8 and *Tri8* removes the acetyl group at carbon 3 to generate 15-acetyldeoxynivalenol (15-ADON) (Alexander, 2011). 3-ADON is defined by the acetyl group on carbon 3, instead of carbon 15. The T2 toxin produced by the sister species *F. sporotrichiodes* does not contain a carbonyl group at the C-8 position. Instead, *Tri1*-encoded cytochrome P450 catalyzes the formation of a hydroxyl group at the C-8 position. In addition, an acetyl group is removed from the C-3 of the T2 toxin (McCormick and Alexander, 2002).

The majority of biosynthetic enzymes that catalyze the formation of DON exist as 12 genes on the main trichothecene or the *Tri*-cluster on chromosome 2, initiating with the cyclization of the sterol precursor farnesyl pyrophosphate (FPP) (Kimura *et al*., 2003; Kimura *et al*., 2007). The FPP precursor is synthesized via the mevalonate primary metabolic pathway that uses acetyl-coA as a substrate. The other genes are outside this cluster on chromosome 4 including *Tri101* and the two genes on chromosome 1 includes *Tri1* and *Tri16* (Gale *et al*., 2005; Lee *et al*., 2008).

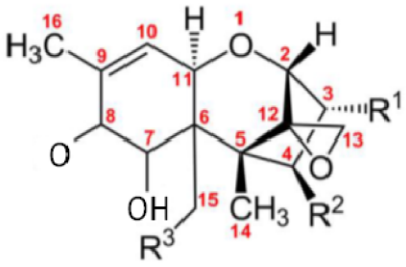

TCTB: Groups present in the R1, R2 and R3 position, respectively:
deoxynivalenol (OH, H, OH)
nivalenol (OH, OH, OH)
fusarenon-X (OH, OAc, OH)
3-acetyldeoxynivalenol (OAc, H, OH)
15-acetyldeoxynivalenol (OH, H, OAc)

Figure 3: Trichothecene B (TCTB) structure and functional groups, from Pinton, *et al*., 2014. © 2014 by the authors; licensee MDPI, Basel, Switzerland.

Mutant studies of genes involved in the biosynthesis of DON have shown that it is the main contributor of disease spread in wheat (Rudd *et al*., 2001; Seong *et al*., 2009; Nasmith *et al*., 2011). Since DON is involved in disease spread, any genetic factor that augments the expression of components in the DON biosynthesis pathway will correspondingly affect pathogenicity. Initial evidence came from deletion of the trichodiene synthase gene *Tri5*, which results in disease mitigation on wheat (Proctor *et al*, 1995). Since then, microscopy studies have shown that a *tri5* mutant is unable to access the rachis, thus blocking access to the vasculature (Jansen *et al*., 2005).

The Tri6 and Tri10 transcription factors are key regulators of genes of the trichothecene biosynthetic gene cluster (Gardiner *et al*., 2009). Targeted deletion of *Tri6* and *Tri10* resulted in localized necrosis and colonization at the site of inoculation and the fungus was unable to migrate and cause symptoms past this point (Seong *et al*., 2009; Nasmith *et al*., 2011). Tri6 is a Cys_2His_2 zinc finger transcription factor and positively regulates the expression of the other *Tri* genes (Seong *et al*., 2009). DNA microarray analysis showed that ~ 200 genes were altered in *ΔTri6* or *ΔTri10* mutants (Seong *et al*., 2009). Moreover, a chromatin immunoprecipitation analysis with Tri6 indicated that in addition to the genes of the *Tri* cluster, Tri6 also regulates genes involved in primary metabolism, most notably the genes of the branched chain amino acid (BCAA) (Nasmith *et al*., 2011, Subramaniam *et al*., 2015, Mol Micro in press). Recent studies showed that genes involved in the BCAA metabolic pathways contribute both to DON production and virulence (Liu *et al*., 2015).

1.5 Factors influencing DON biosynthesis and FHB disease

Biosynthesis of secondary metabolites originates from products derived from primary metabolism. Research in the past decade has seen an explosion in the numbers of genes that regulate the production of DON in *F. graminearum*. Genes that affect DON production are diverse. For example, mitogen activated protein kinases (MAPK) Map1 and Mgv1 have been implicated in DON production. Interestingly, mutations in the respective kinase also show defects in specific developmental pathways. For example, deletion of *Map1* resulted in reduced vegetative growth and the inability to form perithecia, but retained its ability to form the asexual conidiophores. Overall, there was a reduction in virulence (Urban *et al*., 2003). An *mgv1* mutant shows similar defects in sexual development and pathogenicity (Hou *et al*., 2002). Additionally, the mutant also showed increased sensitivity to cell wall degrading compounds, indicating that *Mgv1* is also involved in cell wall biogenesis in *F. graminearum* (Hou *et al*., 2002). Other regulatory proteins that have been found to impact development and influence FHB disease outcome include F-box proteins. These proteins are part of the ubiquitin ligase complex that promotes degradation of regulatory and signalling proteins by the ubiquitin complex (Han *et al*., 2007). A mutation of one F-box gene, *FBP1* resulted in 30% reduction in hyphae growth, similar to the phenotype observed with the aforementioned MAPK mutants (Han *et al*., 2007). Recently, a homologue of *FBP1* in *F. oxysporum* was found to be epistasic to a MAPK and similar to *F. graminearum*. Mutation of this kinase was found to result in both cell growth and cell wall integrity, indicating the high degree of synteny between pathogens (Miguel-Rojas and Hera, 2015).

Analogous to the MAPK signaling modules, genes of the Velvet complex comprise another signaling module that shares similarities with other fungi. The module has provided a foundation for deciphering the mechanism that links secondary metabolite and fungal development (Bayram *et al*., 2008). In *Aspergillus*, where this module has been extensively studied, the Velvet complex consists of at least three proteins that include a light-regulated VeA, and together with LaeA and VelB proteins integrate light, nutrients and developmental signals (Bayram *et al*., 2010). A deletion of a homologue of *VelvA* in *F. graminearum* results in reduced conidiation, aerial mycelia, DON production and correspondingly reduced virulence on wheat (Merhej *et al*., 2012).

In addition to signal transduction pathways, constituents of the cell wall are also emerging as factors essential for pathogenicity. Chitin, which is a polymer of N-acetylglucosamine forms 10-20 percent of the fungal cell wall. Chs5 and Chs7 are two chitin synthases and mutations in these genes result in no perithecia formation and reduced conidia production, as well as defects in cell wall rigidity (Larson *et al*., 2011). One of the interesting observations made was the increased presence of woronin bodies in these mutants (Kim *et al*., 2009). Woronin bodies are organelles that plug septal pores to prevent cytoplasmic leakage. Therefore, increased presence of these structures may suggest that cells are countering the effects of cell wall defects and may function to prevent further structural damage to the cell (Kim *et al*., 2009).

1.5.1 Physiological conditions affect DON production

Physiological conditions that are critical for the regulation of mycotoxin production in *F. gramineraum* include sources of nitrogen and carbon, temperature,

oxidative stress, and extracellular pH (Merhej, *et al*., 2011; Min *et al*., 2012; Min *et al*., 2012(a); Ponts *et al*., 2007; Zhang, 2015). For example, nutrient sources such as nitrogen are important factors regulating secondary metabolism (Woloshuck, 2013; Kim, 2008). In *Fusarium*, the presence of non-preferred nitrogen sources such as agmatine induces the expression of toxin related genes, whereas preferred sources such as ammonium repressed expression (Gardiner *et al*., 2009). This is supported by transcriptome analysis of *F. graminearum* during infection in wheat that showed up-regulation of many genes involved in nitrogen metabolism (Lysøe *et al*., 2011). A transcription factor, AreA has been identified as a critical protein that coordinates many genes governing utilization of nitrogenous compounds (Hou *et al*., 2015). In *F. graminearum*, deletion of *AreA* reduces the fungus's ability to infect wheat and diminishes trichothecene biosynthesis (Giese *et al*., 2013). A recent study showed that Tri10, one of the regulatory proteins involved in the mycotoxin biosynthesis pathways in *F. graminearum* co-immunoprecipitated with AreA (Hou *et al*., 2015). This links genes involved in nitrogen metabolism to secondary metabolism in *F. graminearum*.

Another example is the adaptation to environmental pH conditions. Studies in *Aspergillus nidulans* suggests that Pac1, a zinc finger protein, is the key regulatory factor that detects changes in pH (Peñalva *et al*., 2008). In *F. graminearum*, low pH triggers that activation of the *Tri* genes and consequently the production of mycotoxin (Gardiner *et al*., 2009; Merhej *et al*., 2010). Similar to *A. nidulans*, a *Pac1* homologue in *F. graminearum* also acts as a sensor for pH changes (Merhej *et al*., 2011). A targeted deletion of *Pac1* (*FgΔpac1*) resulted in increased trichothecene production, suggesting that this protein acts as a repressor of genes expressed under acidic pH conditions

(Merhej *et al*., 2011). Moreover, the mutant also showed increased sensitivity to oxidative stress (Merhej *et al*., 2011).

1.6 Role for reactive oxygen species in fungal development and pathogenicity

In the last few years, it has become evident that reactive oxygen species (ROS) plays an important role in both development and pathogenesis in various fungi (Heller, 2011). ROS can be produced actively by enzyme complexes such as NADPH oxidase (NOX) or as products of metabolism in mitochondria or peroxisomes (Heller and Tudzynski, 2011). The NOX complex, initially identified in human phagocytic cells, generates superoxide as part of the neutrophil oxidative burst defense response (Tudzynski *et al*., 2012). This enzyme transfers electrons across the cell membrane and allows for the reduction of molecular oxygen to superoxide. Superoxide dismutase then promotes the dismutation of superoxide to hydrogen peroxide (H_2O_2). This species is also more stable and can pass freely through membranes. Studies suggest that H_2O_2 at certain levels is important in signal transduction. Since it is efficiently produced and translocated, it functions in both local and distant signaling in a cell (Yang *et al*., 2012).

Fungi, including *F. graminearum* have three NOX isoforms where NOXB is similar to NOXA, however it has an extension of 40 amino acids at its N-terminus (Malagnac *et al*., 2004). This N-terminus portion is not present in NOXC, which instead has an EF-hand motif thought to be involved in calcium binding (Kawahara, 2007). The NOX complex also consists of several cytosolic components that are required for its activity at the plasma membrane. In fungi, only two components of the NOX complex

have any homology to its mammalian counterpart. NOXA is equivalent to the mammalian/plant gp91^{phox}, the catalytic center of the NOX enzyme and Rac2, a GTPase that is proposed to interact with the NOX enzyme activation domain (Takemoto, 2007). Recently, the p22^{Phox} subunit, also called NOXD, was found in *Magnaporthe grisea* and is hypothesized to function as a cell wall recruited glycoprotein required for NOX complex formation (Lacaze *et al*., 2015).

The NOX signaling system has impact on a range of functions in varieties of fungi. One of the first fungi, where NOX was examined in detail was in *Aspergillus nidulans*. Specifically, *NOXA* was found to be essential for formation of sexual fruiting bodies. Deletion of *NOXA* resulted in a decrease in superoxide production in early sexual structures (Lara-Oritz *et al*., 2003). In *Botrytis cinerea*, deletion of both *NOXA* and *NOXB* caused a reduction in virulence and sexual development, but did not cause an alteration in the production of superoxide (Segmüller *et al*., 2008) In the ascomycete, *Podospora anserina* NOX1 (similar to NOXA) was shown to be essential for aerial hyphae development and differentiation of ascogonia to ascospores (Malagnac *et al*., 2004). Furthermore, it has been found that pathogenicity also depended on a functional NOX complex. In *Magnaporthe grisea, NOXA* and *NOXB* mutants fail to infect rice due to a defect in appressorium formation (Takemoto *et al*., 2007).

A recent study in our lab led to the characterization of *NOXA* and *NOXB* in *F. graminearum*. The results showed distinct features of each *NOX* gene. While the *NOXA* mutant was unable to make perithecia, only the double mutant (*ΔNOXA/B*) resulted in the reduction of pathogenicity in the fungus (Wang *et al*., 2014). Interestingly, the *ΔNOXA/B* strain is still able to produce 15-ADON in culture, levels similar to wildtype. These

results indicated that *NOXA* and *NOX*B are similar; yet, they possess distinct activities associated with specific phenotypes. It is not known how these distinct features are formulated at the cellular level. It is proposed that these two enzymes may interact with common proteins to perform the enzymatic function or interact with distinct proteins to perform their unique roles in a cell.

1.7 "Redox" proteomics to find targets of the NOX complex

The "redox proteome" is a set of proteins in which cysteine residue(s) are specifically oxidized in a reversible manner (McDonagh *et al*., 2009). At biological pH, cysteine is represented as a thiolate anion (S−) and if there are cysteine residues in close proximity to each other, they can share the charge, combining to form a strong disulfide bond in proteins (Brandes *et al*., 2009). The H_2O_2 oxidization of a single thiolate anion to the sulfenic form (SO−) can also change the charge of the region and thus modify protein conformation and activity (Reczek and Chandel, 2015). One example of cellular use of an oxidant-sensitive cysteine residue is in the *Saccharomyces cerevisiae* transcriptional regulatory protein Yap1 (Kuge *et al*., 1997). This transcription factor (TF) has a cysteine-rich domain at both the N and C termini of the protein. In the presence of H_2O_2 , a disulfide bond occurs between these two terminals, resulting in a structural change, which hides the nuclear export signal in the C-terminus such that the TF is retained in the nucleus and promotes the transcriptional activation of genes involved in the antioxidant response (Delaunay *et al*., 2000; Gulshan *et al*., 2005).

One of the methods to identify proteins that have redox sensitive cysteines uses a proteomics approach. As described in Figure 4, the procedure involved blocking free

thiols with iodoacetamide when cells are lysed in denaturing buffer (Step 1). DTT (dithiothreitol) is applied to reduce reversibly modified thiols followed by labelling of with biotin-HPDP ([hexyl]-3-(2-pyridyldithio) propionamide) (Steps 2 and 3). Tryptic digestion of proteins precedes biotinylation and isolation on a streptavidin column (Steps 4 and 5). Biotinylated peptides are eluted from the column using β-mercaptoethanol, followed by sequencing via LC MS/MS (Step 6). By using a method to directly tag proteins, one can with confidence, identify the subset of proteins that are susceptible to reversible oxidation at the cysteine residues (McDonagh *et al*., 2009). Since the NOX complex is associated with various functions, proteins regulated by the production ROS is of great interest in biology (Ghezzi *et al*., 2005). Our current understanding of fungal proteins that are reversibly modified through redox modification is limited, and thus dissecting the role of 'redox' proteins is of interest.

1.8 Thesis Outline

My thesis in part examines the 'redox' status of proteins in *F. graminearum* during stress conditions. These conditions are conducive for the activation of pathogenicity factors such as DON. The redox status of proteins from the wildtype *F. graminearum* was compared with the *NOXA/B* double mutant strains, which allowed us to identify proteins that are directly affected by the NOX protein complex. The "redox proteome" was generated by Dr. Chris Rampitsch using a gel-free affinity-enrichment strategy. This purification strategy in combination with a triple TOF (time of flight) mass spectrometry technique allowed for quantitative characterization of the 'redox' proteins.

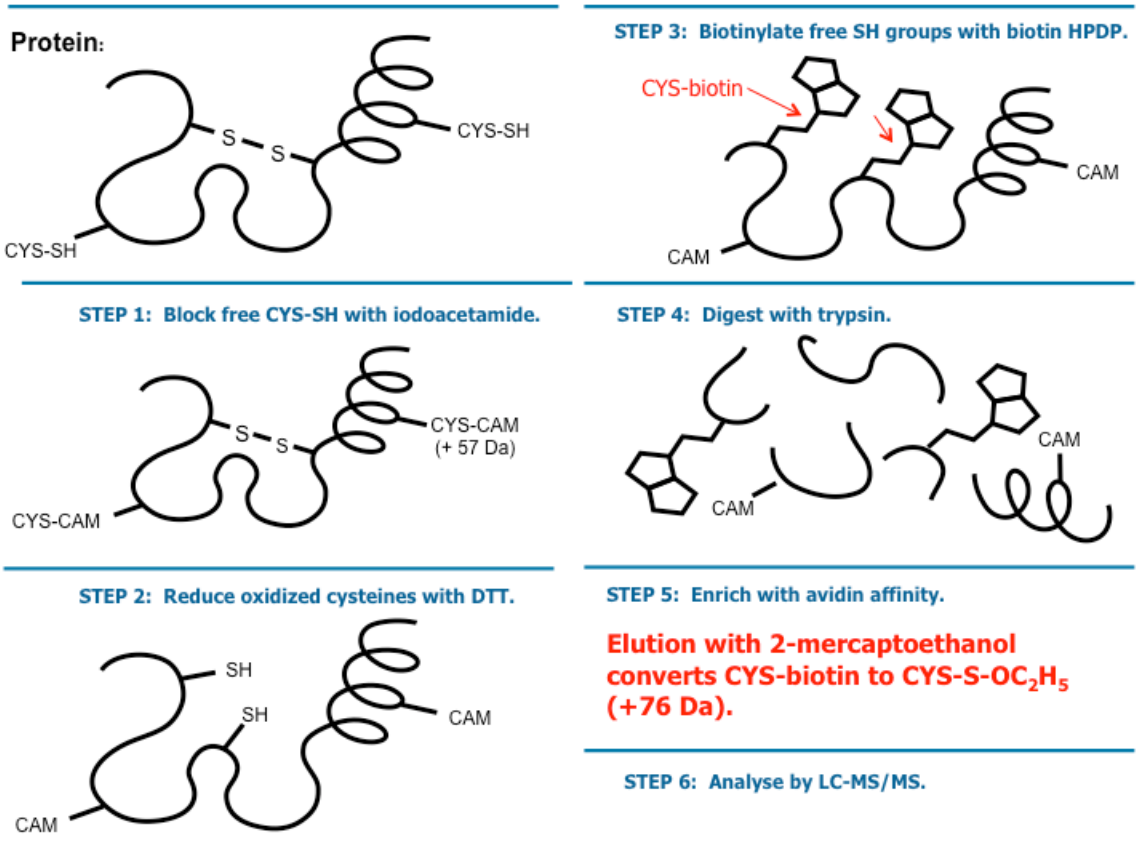

Figure 4: Isolation of proteins involved in di-sulfide bonds for analysis by mass spectrometry (Modified from Joshi M, 2011)

Chapter 2- Materials and Methods

2.1 Fusarium strains, propagation and storage

F. graminearum DAOM 233423 was used as the wildtype strain and all transgenic strains were created using this strain. Mycelia were propagated on solid PDA (potato dextrose agar) agar plates. Spores were grown by inoculating a plug of agar/mycelia into 25 mL of CMC liquid media for 3 days (Cappellini and Peterson, 1965). Spores were isolated by filtration on miracloth, followed by two washes in sterile water, centrifuging at 5000 rpm for 5 minutes each time. For the diurnal zonation assay a fresh plug of mycelia was plated on a carrot agar plate, and subject to a cycle of 12 hours day and 12 hours night for 4-5 days or until mycelia reaches the edge of the plate (Leslie and Summerell, 2006). Strains were stored in 15% glycerol at -80ºC as mycelial plugs derived from SNA medium. All strains are deposited at the Canadian Collection of Fungal Cultures at Agriculture and Agri-Food Canada (Ottawa).

2.2 Generation of the redox proteome

2.2.1. Protein extraction

Three biological replicates of both *F. graminearum* (*Fg*) WT and *Fg* Δ*noxA/B* cultures were grown for comparative proteomic analysis. Harvested fungal tissues were ground in liquid nitrogen using a mortar and pestle. Six-hundred mg of ground tissue were suspended in 8 mL of extraction buffer (10% w/v trichloroacetic acid (TCA), without dithiothreitol (DTT), in cold acetone) and incubated at -20°C for 2 hours for protein precipitation. The samples were centrifuged at 14,000 x g for 20 minutes at -5°C. The pellet was washed with 8 mL of ice-cold acetone, without DTT, and centrifuged as

before. After repeating five acetone washes, the final pellet was dried under a stream of nitrogen gas and stored at -80°C. Proteins were quantified using the Bradford dye-binding assay (Bio-Rad Laboratories, Hercules CA, USA) with BSA as standard.

2.2.2 Protein alkylation and reduction

Detection of proteins with cysteine residue(s) oxidized in a reversible manner is based on their reducibility by DTT, after blocking the free cysteine(s) with an alkylating agent. 600µg of proteins were suspended in denaturing buffer (8 M urea, 4% CHAPS, 2 mM EDTA and 50 mM Tris–Cl pH 8.0) with 100 mM final concentration of IAA (LeMoan *et al*, 2009). The alkylation reaction was carried out in dark for 30 min. Excess DTT (40 mM) was used to reduce the disulfide linkages as well as quench unused IAA. Samples were incubated for 45 minutes on a rotator at room temperature. Proteins were precipitated with TCA/acetone as before and washed with acetone to remove remaining DTT.

2.2.3 Gel-free with biotin-affinity chromatography

DTT-reduced cysteine(s) were tagged with 0.5 mM biotin-HPDP (Pierce, Biotechnology) using manufacturer's instructions and incubated on a rotator in the dark for 45 minutes (McDonagh *et al*, 2009). Samples were precipitated again with TCA/acetone and washed with acetone to remove any excess biotin-HPDP. Pellets were re-dissolved in 200 µl of 50 mM ammonium bicarbonate and a 5 µl aliquot was taken to measure protein concentration in samples using Bradford assay. One-hundred µg of

protein was digested with trypsin (Promega) at a ratio of 1:100 (wt:wt) trypsin:protein and incubated at 37°C for 2 hours.

2.2.4 Selective isolation and enrichment of redox sensitive cysteines

Streptavidin–Agarose CL-4B resin (Sigma-Aldrich) was prepared by washing twice in binding buffer (4 M urea, 2% (w/v) CHAPS, 50 mM NaCl and 25 mM Tris–Cl, pH 8.0) and 25 µl of this slurry was incubated with peptides for 2 hours at room temperature. Following incubation, the resin was washed once with binding buffer, twice with wash buffer A (8 M urea, 4% (w/v) CHAPS, 1 M NaCl and 25 mM Tris–Cl, pH 8.0) and three times with wash buffer B (8 M urea, 4% (w/v) CHAPS and 25 mM Tris–Cl, pH 8.0). Urea was removed by washing the resin four times with wash buffer C (5 mM ammonium bicarbonate, 20% (v/v) acetonitrile). Biotinylated peptides were eluted from the resin by adding 25 µl of wash buffer C containing 5% (v/v) β-mercaptoethanol and incubated at 90°C for 3 minutes. Peptides were collected by centrifugation and analyzed by LC-MS/MS.

2.2.5 LC-MS/MS analysis

Tryptic peptides from biotin-affinity chromatography were analyzed by a linear ion trap mass spectrometer (LTQ XL: Thermo Fisher, San Jose, CA) connected on-line with a nano-HPLC (UltiMate^{TM}3000: Dionex, Germany). A 10 cm C_{18} column (5 µm particle/ 300 pores) was prepared in-house and used to introduce peptides into the mass spectrometer via nanospray ionization at 250 nL/min using a 2–80% v/v ACN gradient in 1% v/v formic acid, 0.5% v/v acetic acid over 20 min. The mass spectrometer was

operated in positive ion mode with source temperature 200°C and tuned in nano-spray mode using 10 µM (Glu-) Fibrinopeptide B (GluFib) singly charged ion at *m/z* 1552.67. A full survey scan (MS) was acquired over 400– 2000 m/z range. MS/MS data were acquired in data dependent scan mode, using a "Big Five" program that selects the five most intense ions for fragmentation, with dynamic exclusion set to 120 sec. In all cases, a nESI spray voltage of 1.8 kV was used.

2.2.6 Database search and assignment of redox sensitive cysteines

CID (collision induced dissociation) fragmentation spectra were searched against an *F. graminearum* protein database using MASCOT (v2.2, Matrix science, UK) (Perkins *et al*, 1999). Proteins were identified through sequence similarity search with BLASTP against the non-redundant sequence database at National Centre for Biotechnology (NCBI). Peptide mass tolerance was set to ±2 Da, fragment mass tolerance was ±0.8 Da, and up to 1 missed tryptic cleavages were allowed. Monoisotopic peptides with charged states of +1, +2 and +3 were queried using using b- and y-ion series; Decoy searches, which queried the reversed database, were included in all searches.

Peptides from biotin-affinity chromatography were searched using variable modifications. The "β-mercaptoethanol" adduct brings a modification of +76 Da at cysteine residues and was added as a variable modification with an elemental composition of $C_2 H_5 SO$. The following criteria were used to determine whether cysteine modified peptide assignment had been performed correctly. All peptides with an ion score greater than the significance threshold (i.e. $p<0.05$) were considered. The ions

score is −10 log(*P*), where *P* is the probability that the observed match is a random event. Individual ions scores >48 indicated identity or extensive homology**.**

2.3 Bioinformatics

Protein sequence paralogs were identified using NCBI BLAST (basic local alignment search tool) (http://blast.ncbi.nlm.nih.gov/Blast.cgi). Multiple sequence alignment was completed using MUSCLE (**MU**ltiple **S**equence **C**omparison by **L**og-**E**xpectation)(http://www.ebi.ac.uk/Tools/msa/muscle/). Identification of Signal sequence was identified with Signal P (http://www.cbs.dtu.dk/services/SignalP/). Identification of targeting location was done with Target P (http://www.cbs.dtu.dk/services/TargetP/) . The prediction of the gpi anchor was confirmed with the "big-PI Fungal Predictor" (http://mendel.imp.ac.at/gpi/fungi_server.html)

2.4 Generation of *F. graminearum* transgenic Strains and fungal transformation

2.4.1 Generation of *ΔFGSG_10089*

The deletion construct of *FGSG_10089* was accomplished by PCR amplification of the two homologous recombination sequences (HRS) with primer set O1/O2, which amplified the promoter of FGSG_10089 (FGSG_10089p) and primer set A2/A3, which amplified 3' flanking region of *FGSG_10089* (FGSG_10089 3') (Figure 7). The two HRS products FGSG_10089p and FGSG_10089 3' were introduced into the pRF-GU2 vector, which is a modified version of the pRF-HU2 vector, where a Geneticin selection marker replaced the Hygromycin selection marker (Figure 7) (Frandsen *et al*., 2008).

Deletion of the gene was verified by PCR using gen F / gen R primers detecting the presence of the geneticin marker, and FGSG_10089 F / FGSG_10089 R primers verifying the absence/presence of the coding region (Figure 7d).

2.4.2 Generation of overexpression strains

The Δ*FGSG_10089*-FGSG_10089 overexpression strain was made using the Gateway© cloning system (Life Technologies). The coding sequence (CDS) of FGSG_10089 was amplified (O2/O3) using PfuTurbo Cx Hotstart polymerase (Stratagene) and cloned into the pSW-GUE vector, which contains the promoter for glyceraldehyde-3-phosphate dehydrogenase (pGpd), using the USER (Uracil-Specific Excision Reagent) cloning (New England Biolabs, USA) procedure.

2.4.3 Generation of point mutation strains

Point mutations in FGSG_10089 were constructed with the *FGSG_10089* gene cloned into pENTR/ dTOPO. Two primers, (Fg 10089 int MF/R) (Appendix, Figure 1), complementary to each other were designed with point mutations in the codon, so that the cysteine residue was changed to amino acids serine and phenylalanine, respectively upon amplification with PCR. PCR products were digested with 1 μL of Dpn1 enzyme and an aliquot was transformed into *E. coli* DH5α. The mutations were confirmed by sequencing and cloned into the overexpression vector, pSW-GUE as described before.

2.4.4 Generation of complementation strains

To express *FGSG_10089* with the native promoter, the promoter was amplified using FGSG_10089proF/R primers, with FGSG_10089proF with an overlap of the *FGSG_10089* CDS. A second PCR product was created by amplifying the CDS of the WT *FGSG_10089* and the point mutant clones. Finally, a fusion PCR product was created by combining the two PCR products with the USER overhang primers (FG10089-native FWD/REV_USER). Each fusion product was verified using O1/O3 primers (Fwd1_FG10089user_promoter/ REV3_FG10089cds_user) (Figure 7). The fusion PCR products were inserted into the pRF-GU vector using the USER reaction (New England Biolabs, USA). All of the genetically altered strains were generated by *Agrobacterium*-mediated transformation (Frandsen *et al*., 2008). The list of primers can be found in Appendix Table 1.

2.5 Trichothecene analysis by HPLC

To induce trichothecene production in liquid culture, a modified two stage media protocol was employed (Nasmith *et al*., 2011). A nylon net filter was added to the culture plates. This allowed for even growth and avoided mycelia clumps (Walkowiak *et al*., 2015). Briefly, 2 x 10^4 spores of wild type and mutant *F. graminearum* strains were inoculated into 4 mL of nutrient-rich media for 48 hours and washed twice with water. The mycelial mass was suspended in 4 ml of mycotoxin-inducing media (1g $(NH_4)_2HPO_4$, 3 g KH_2PO_4, 0.2 g $MgSO_4 \cdot 7H_2O$, 5 g NaCl, 40 g sucrose, 10 g glycerol in 1 L, pH 4.0) and then transferred to the 6-well culture trays. The supernatant was collected after 48 hours for trichothecene analyses and the mycelial solids were collected by

filtration and washed twice in water and stored at -80˚C for RNA analyses. Trichothecenes were analyzed by HPLC with direct injection of 100 µL of the culture filtrate into a 150 x 4.6 mm 5 µm Hypersil ODS column (Thermo-Fisher, Canada), using an isocratic methanol: water gradient at 15% over 25 min at a flow rate of 1 ml/min. Trichothecenes were monitored by UV 220 nm and the concentration of 15-ADON was calculated based on a dilution curve derived from pure 15-ADON standard (Nasmith *et al*., 2011).

2.6 DNA extraction and PCR

DNA from wild type and mutant *F. graminearum* strains were isolated from mycelia grown on a fresh PDA plate with the E.Z.N.A Fungal DNA mini kit. Briefly, mycelia were ground in a screw cap microcentrifuge tube using the Bertin Precellys 24 Homogenizer. PCR reaction consisted of 0.2 uM forward primer, 0.2 uM reverse primer, 0.2 mM dNTPs, 1X PCR buffer and 25 ng of DNA template.

2.7 RNA isolation and quantitative Real-Time PCR

The mycelial pellet isolated from the mycotoxin-inducing media was flash frozen in liquid nitrogen prior to RNA isolation. RNA was isolated by Trizol (Invitrogen, Carlsbad, CA, U.S.A.) and purified by InviTrap Spin Cell RNA Mini Kit (Invitek, Berlin, Germany). RNA was converted into cDNA by the Applied Biosystems cDNA synthesis kit according to the manufacturer's instructions (Applied Biosystems, Canada). All of the qRT-PCR reactions were performed with three technical replicates using the Applied Biosystems Power SYBR Green kit (Applied Biosystem, Canada) and the Applied

Biosystems StepOne Plus Real-Time PCR System according to manufacturer's instructions (Applied Biosystems, Canada). For relative quantification (RQ), a standard curve for each primer set was created. β-tubulin (*FGSG_09530*) was used as the internal standard between samples. The data was imported and analyzed in StepOne 2.1 software.

2.8 Pathology tests and analyses in *Triticum aestivum* (wheat)

The susceptible variety of wheat 'Roblin' was grown in growth chambers until anthesis was reached as described in Schreiber *et al*. (2011). At mid-anthesis, the plants were inoculated between the palea and lemma with approximately 1,000 conidia. Inoculated plants were transferred to a contained misting facility and monitored for the development of disease symptoms such as spikelet discoloration. Data was collected when heads in the control treatment group exhibited approximately >90% infection. Students t-test was performed to assess any differences between the wildtype and transgenic strains

2.9 Maintenance and storage of *S. cerevisiae* strains and transformation

S. cerevisiae strain BY4741 was used as the wild type strain. The strain is haploid mating type designated "Mat a". For long term storage purposes, cells were propagated in YPD (Yeast Extract Peptone Dextrose) at 30°C shaking at 200 RPM overnight and diluted with glycerol to 15%. Yeast knockout strains were transformed with the *FGSG_10089* and expressed in pYES-DEST52 using the following procedure (Amberg, 2005). The culture was grown to OD_{600} = 0.6 and centrifuged at 3000 rpm for 2 minutes. The pellet was washed in 0.1M Lithium Acetate (LiAc) in TE and centrifuged as before

and suspended in 350 µl of ddH_2O. A 100 µl aliquot was used for transformation was added to a tube containing 240 µl 50% PEG 3350 (w/v), 36 µl 1 M LiAc, 50 µl boiled salmon sperm carrier DNA (2 mg/ml), and 34 µl digested plasmid DNA. The mixture was incubated at 30ºC for 30 minutes, heat shocked at 42ºC for 15 minutes, centrifuged at 2500 rpm for 1 minute. PEG-LiAc was removed and washed with sterile ddH_2O followed by centrifugation at 2500 rpm for 1 minute. The pellet was resuspended in YPAD and recovered in 5ml of YPAD for 3-4 hours and plated on YPD + Geneticin.

2.10 Protein induction, Western blot and complementation assay

To induce the expression of *FGSG_10089* in pYES-DEST52, a single colony was inoculated into 5 ml of YPD overnight. A 100 µL aliquot of the overnight culture was inoculated in 5 mL of medium containing 2% raffinose and grown overnight at 30º C with shaking. A 300 µL amount of culture was added to induction media (without uracil and containing 2% galactose), grown at 30°C with shaking for 24 hours. One mL aliquot was centrifuged at 3800× g for 5 min and washed twice, flash frozen in liquid nitrogen and stored at -80 °C. To extract the protein, the yeast pellet was resuspended in 100 µL lysis buffer (8 M urea, 0.1 M NaOH, 0.05 M EDTA, 2% SDS, 2% β-mercaptoethanol, Roche Complete Protease Inhibitors) and lysed in a Fast-Prep Machine (MP biomedicals) for 45 sec. The sample was heated to 55°C for 10 minutes and neutralized with 2.5 uL of 4M acetic acid. The sample was placed in a 55°C water bath for 10 minutes and the protein lysate was cleared by centrifugation, at 12,000 rpm for 5 minutes. A 25 uL loading buffer was added to 20 µL supernatant and denatured at 95 °C prior to loading on a Bio-Rad pre-cast gradient gels (Bio-Rad).

The FGSG_10089 protein was detected by Western blot analysis by transferring the gel onto a PVDF membrane using the Trans-Blot® Turbo™ Transfer System (BioRad). Briefly, the membrane was blocked for non-specific sites with 1% Roche blocking reagent for one hour, followed by 5 x 5 minutes washes in TBST + 0.1% tween 20. The His C-terminal HRP antibodies (Invitrogen) was used to detect FGSG_10089 protein with ECL imaging solution (Bio-Rad).

The complementation assay was done on CFW (calcofluor white-YPD-2% galactose) plates following the protocol as detailed by Ram and Klis (2006) with yeast cells that were induced as described before.

2.11 Confocal microscopy for cell wall analysis

Confocal microscopy was conducted with the help of Denise Chabot (AAFC, Ottawa). Freshly grown mycelia and conidia of WT and Δ*FGSG_10089* were resuspended in CFW (0.07% in 0.1M $NaPO_4$ pH 8) and put onto a glass slide. A Zeiss LSM Duo 510 confocal microscope with ZEN 2009 software was used to image the mycelia and conidia. Epifluorescence was imaged with a Zeiss Filter #1 (full range of colors). CFW was excited with laser 405 nm and emission was recorded with BP 420-490 nm. The DIC channel was used for all of the observation (Objective -Alpha Plan Apochromat 63X/1.46)

Chapter 3- Results

3.1 Identification of redox targets of *NOX*

All protein isolation procedures and MS analyses were conducted by Dr. Chris Rampitsch (AAFC, Morden).

Based on the phenotypes observed with the NOX double mutant, Δ*NOXA/B*, it is apparent that NOX enzymes are involved in the regulation of a variety of cellular functions that control important developmental pathways and pathogenicity (Wang *et al.*, 2013). Thus, identification of proteins modified by ROS generated by the NOX enzyme is a necessary step to elucidate targets contributing to pathogenicity. Although there are several types of oxidative modifications, we chose to focus on cysteine-thiol oxidation that causes disulfide formation and a structural change within proteins.

To simulate the induction of virulence factors *in-vitro*, the wildtype strain (WT) and Δ*NOXA/B* were grown in a nitrogen-limiting medium and the redox proteome was analyzed in triplicate over a time course at 0, 4, 6, and 24 hours. Differentially modified proteins between the two strains were determined by gel-free enrichment of peptides followed by mass spectrometry. Gel–free enrichment of peptides involves reduction with DTT and tagging with biotin, which allowed peptides to be purified on a streptavidin column (Figure 4). Differences between WT and the Δ*NOXA/B* mutant were determined by generating a ratio of protein cysteine-thiol oxidation between strains. A ratio > 1.0 would indicate that the protein is more oxidized in WT.

As indicated in Table 1, 16 proteins were identified that were differentially modified between WT and Δ*NOXA/B* mutant. Functional characterization by the Munich

Information Center for Protein Sequences (http://www.helmholtz-muenchen.de/en/ibis/institute/groups/fungal-microbial-genomics/resources/fgdb/index.html) revealed potential functions of putative targets of NOX A/B enzymes (Ruepp *et al*., 2004). Of the 15 annotated proteins, 11 are involved in metabolism and are part of glycolysis (FGSG_01346, FGSG_02770, FGSG_05454), TCA cycle (FGSG_05454), biosynthesis of amino acids (FGSG_00421, FGSG_09321 FGSG_09834), as well as the metabolism of nucleotides (FGSG_00421, FGSG_08737), phosphates (FGSG_00421, FGSG_08627), carbohydrates (FGSG_00421, FGSG_01346 FGSG_02022, FGSG_02770, FGSG_04826, FGSG_05454, FGSG_09834) and fatty acids (FGSG_02022 FGSG_04826 FGSG_09321). The remaining four proteins were annotated as a heat shock protein (FGSG_06246), involved in development (FGSG_10089), protein synthesis (FGSG_00798 and FGSG_08737), and protein fate (FGSG_06246). To determine if the 16 putative targets of NOXA/B contribute to the observed phenotypes in Δ*NOXA/B*, reverse genetics was used to generate disruption strains of select genes (Subramaniam, unpublished). As indicated, of the seven genes that were targeted for disruption, only 3 were recovered as positive deletions (Table 1). The other four could not be recovered, likely due to the fact those genes are essential and any disruption will lead to lethality. Genes with deletions included *FGSG_10089, FGSG_08737* and *FGSG_09834*. One of the mutants, Δ*FGSG_08737* is unable to produce perithecia and is reduced in virulence, similar to the *NOXA/B* mutant. The mutant Δ*FGSG_09834* did not show any changes in pathogenicity (Subramaniam, Wang, unpublished). The focus of my thesis was characterization of one putative target of

NOXA/B. The following sections will describe detailed characterization of *FGSG_10089*.

Table 1: Cysteine-redox-responsive proteins identified through Gel-Free MS/MS QTOF

FG ID	*W/N_t				Function	Confirmed deletion	Phenotype
	0h	4h	6h	24h		No;ectopic	–
FGSG_00421	1.00	0.96	1.25	1.56	methionine adenosyltransferase	ND[A]	–
FGSG_00798	1.85	1.13	0.91	0.83	ribosomal protein S21 (CRP7)	ND	–
FGSG_01346	0.93	1.00	0.56	0.95	enolase	ND	–
FGSG_02022	0.88	1.26	1.67	1.30	1,3-beta-glucanosyltransferase	No;ectopic	–
FGSG_02770	1.04	1.41	0.80	1.07	fructose-bisphosphate aldolase	No;ectopic	–
FGSG_04826	2.00	1.38	0.33	0.60	mannitol dehydrogenase	Done by Trail,Francis	Expressed early in perithecia development and during wheat infection (Trail, 2009)
FGSG_05454	0.97	0.65	0.53	0.95	pyruvate dehydrogenase E1 component	ND	–
FGSG_06246	0.59	0.85	0.62	0.77	acyl-protein thioesterase 1	ND	–
FGSG_06932	0.84	2.87	1.42	0.90	adenosine kinase	ND	–
FGSG_08365	1.38	1.43	0.86	0.89	hypothetical	ND	–
FGSG_08627	1.94	1.00	1.00	1.06	riboflavin Kinase (FMN1)	ND	–
FGSG_08737	1.54	0.47	0.64	0.47	woronin body major protein	Yes	No perithecia, reduced pathogenicity
FGSG_09321	1.60	1.00	1.19	1.05	acetyl-CoA acetyltransferase	ND	
FGSG_09834	1.00	0.69	0.67	1.33	pyruvate decarboxylase	Yes	Not reduced in pathogenicity
FGSG_10089	1.05	1.42	1.17	0.69	sporulation gene SPS2/ECM33	Yes	reduced pathogenicity
FGSG_10297	1.08	0.85	1.05	1.36	NADH-ubiquinone oxidoreductase	No;ectopic	–

*Numbers refer to ratio of oxidized cysteine, WT/*ΔnoxA/B*

[A] Not done

F. graminearum database: http://www.helmholtz-muenchen.de/en/ibis/institute/groups/fungal-microbial-genomics/resources/fgdb/index.html

3.2 *In silico* characterization of FGSG_10089

Since FGSG_10089 has not been previously characterized in the literature, a bioinformatics approach was taken to look for conserved domains and signatures in the protein, which may indicate its function. Signal P, which is a program designed to identify signal peptides (Nielsen *et al*., 1997) identified a signal peptide at amino acids 1-20 with the cleavage site between residues 20 and 21 of the protein, which is supported by the hydrophobicity of these residues, canonical to signal peptides (Figure 5). Target P predicted the protein to be a part of the secretory pathway meaning that it could be targeted to the outside of the cell, or other organelles including the Golgi, ER (endoplasmic reticulum), or lysosome/vacuole (Petersen *et al*., 2011). Further assessment using a GPI-anchor site predictor program, specific to fungi indicated that FGSG_10089 has a GPI site with the omega site at residue 374 (P_{Value}= $5.4e^{-06}$). An examination of the amino acid sequence also confirmed presence of a hydrophobicity tail at the C-terminal domain, which is a signature of the GPI anchor cleavage site (Eisenhaber *et al*., 2004). This confirmed that FGSG_10089 is most likely targeted to be secreted to the outside of the cell wall. Domain analysis using NCBI conserved domain search indicated that residues 212-276 may form a receptor L (ligand)-domain, however, a 50 amino acids domain is absent (P_{Value}= $1.14e^{-04}$). L-domains are known to function within epidermal growth factor receptors (EGFRs) and insulin receptors to bind ligands or proteins found in the extracellular matrix (Garrat *et al*., 1998)

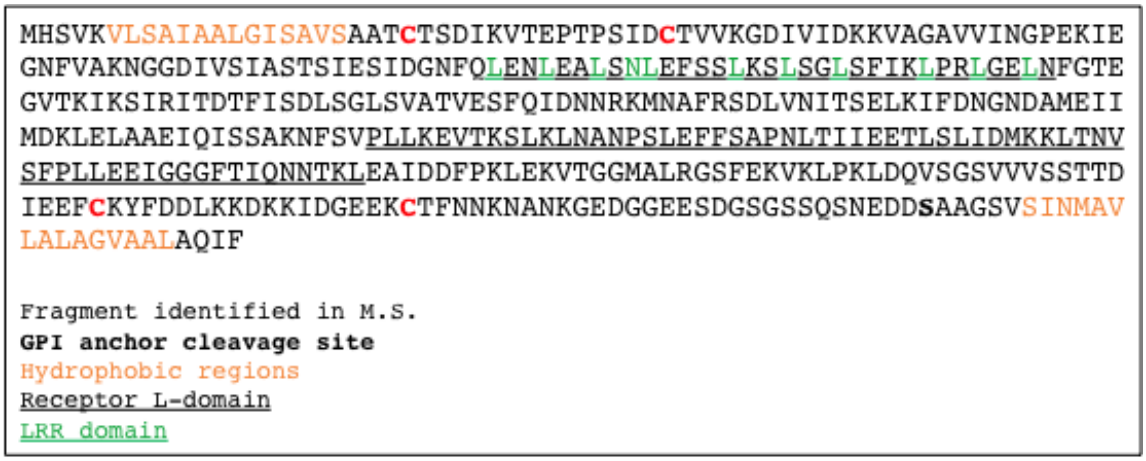

Figure 5: *In-silico* identification of functional domains in the FGSG_10089 protein

FGSG_10089 has not been characterized; however, its function can be predicted from other organisms where an orthologue is present. When we compared FGSG_10089 to the yeast *Saccharomyces cerevisiae* by BlastP, ECM33 was identified as a potential orthologue ($e_{value}=1x10^{-25}$) with 28% identity with 76 % coverage. ECM33 is annotated to have a role in fungal cell wall organization. Similar to FGSG_10089, ECM33 is also cited to have an L-domain and GPI anchor. Alignments determined that FGSG_10089 and ECM33 share many similar residues including conservation of 4 cysteine residues (Figure 6). The oxidized cysteine residue identified by mass spectrometry analyses was at residue 325 (C^{325}), which falls into a region of the protein with no predicted domain. The three other cysteine residues were not found to be modified.

In addition to ECM33, BlastP comparison to *Neurospora crassa*, a filamentous ascomycete, identified ccg-15 with homology to FGSG_10089 ($e_{value}=6e^{-44}$). A study describes the *Neurospora* ccg-15 as a clock regulated a gene, which governs the frequency of reproduction (i.e. sporulation) (Zhu *et al*., 2001; Lombardi and Brody, 2005).

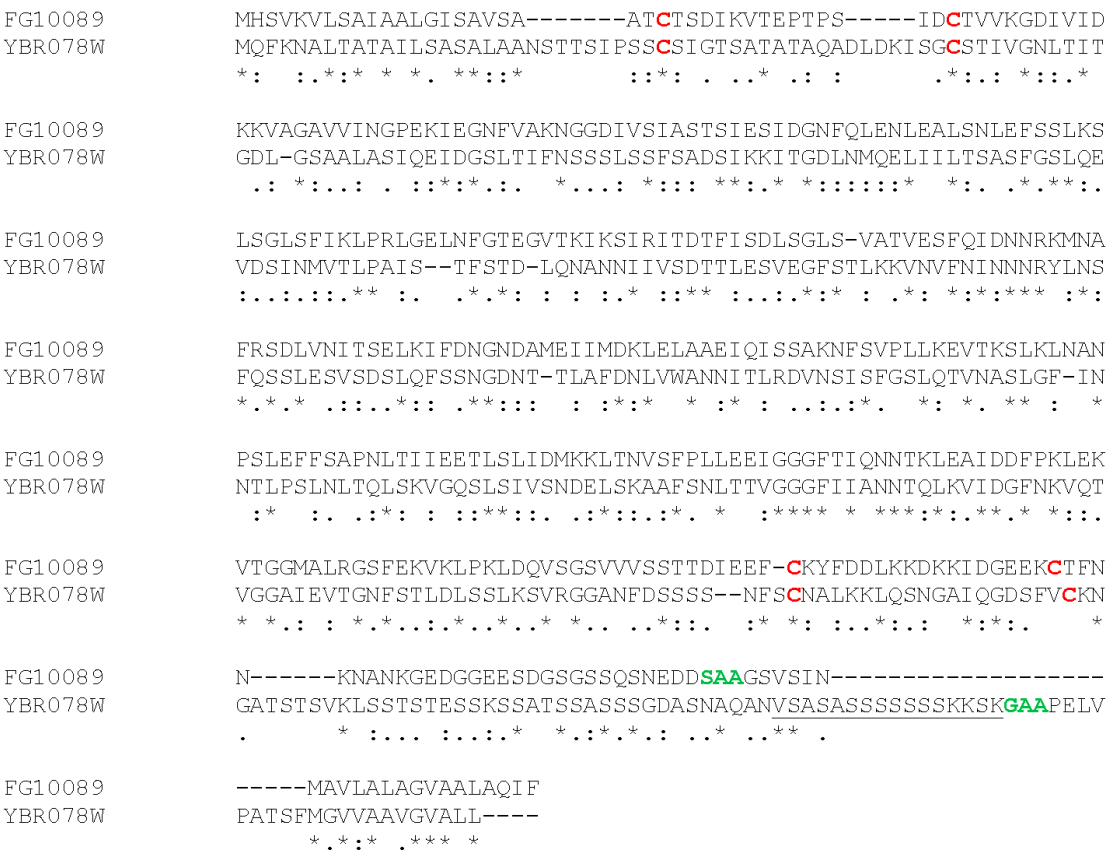

Figure 6: A BLAST search identified that *ECM33 (YBR078W)* from *Saccharomyces cerevisiae* is similar to *FGSG_10089*. The e-value is 3.7×10^{-25} and the coverage is 63%. The 4 cysteine residues are conserved (red). The GPI anchor site in *ECM33* is highlighted in green, preceded by the linker region. The alignment was done with Clustal Omega.

3.3 Generation of disruption, complemented and overexpression strains of *FGSG_10089*

To elucidate the function of *FGSG_10089* in *F. graminearum*, a disruption strain was constructed by targeted gene replacement using pRF-HU2 vector and *Agrobacterium* mediated transformation. The deletion construct of *FGSG_10089* was created by PCR amplification of the two homologous recombination sequences (HRS) with primer set O1 /O2 (Figure 7A) (Frandsen *et al*, 2008). PCR amplification with gene specific primers demonstrated the absence of *FGSG_10089* in Δ*FGSG_10089* deleted strain (Figure 7D, lane 2) compared to the WT control (Figure 7D, lane 1) using primers for the *FGSG_10089* CDS (coding sequence) and *Tri6* primers as a control. Amplification of *FGSG_10089* from the WT positive control showed *FGSG_10089* as a larger product on the gel, due to the presence of introns (Figure 7D, lane 1).

To recover any phenotype observed with the *FGSG_10089* knockout strain, a complement strain (Δ*FGSG_10089* –FGSG_10089) was generated (Figure 7C), where *FGSG_10089* was under the control of native promoter. An overexpression strain (Δ*FGSG_10089* –FGSG_10089$_{overexp}$) was also constructed, where *FGSG_10089* was under the control of the constitutive promoter *gpdA* (glyceraldehyde phosphate dehydrogenase) from *Aspergillus* (Figure 7B). The *Fusarium* transgenic strains were verified by PCR amplification with primers for a region including the gpdA promoter and *FGSG_10089* (Figure 7D, lanes 3, 4,5). The band is absent in lane 1 and 2, indicative of the absence of the overexpression promoter in the knockout and WT strains (Figure 7D).

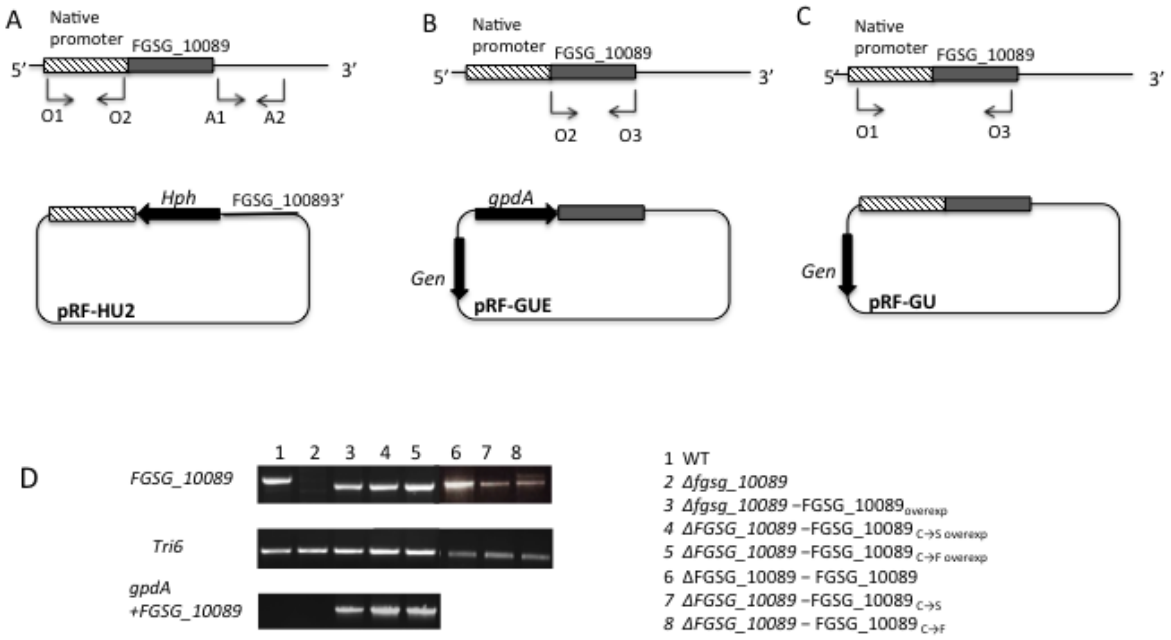

Figure 7: Construction of vectors for knockout (A), overexpression (B), and complementation (C) of *FGSG_10089*. Amplification of knockout and insertion of *FGSG_10089* as well as point mutations to cysteine and phenylalanine are shown in (D), with primers shown to the left. Hph = Hygromycin phospho-transferase expression cassette (selection marker). Gen = Geneticin resistance encoded by the gene Nptl (neomycinphosphotransferase).

3.3.1 Creating point mutation of cysteine residues of *FGSG_10089*

Cysteine 325 (C^{325}) was identified as a target of redox modification, differentially oxidized in Δ*NOXA/B,* compared to WT. To determine the importance and function of the C^{325} in FGSG_10089, two point mutations were created at this residue. The point mutations with C to S and C to F mutation were transformed into Δ*FGSG_10089*, resulted in the $FGSG\_10089_{C\text{-}S}$ strain and $FGSG\_10089_{C\text{-}F}$ strain, respectively using the pSW-GUE vector, confirmed by RT-PCR analysis (Figure 8).

1. WT
2. Δ*FGSG_10089*
3. Δ*FGSG_10089*−FGSG_10089overexp
4. Δ*FGSG_10089*−FGSG_10089 C→$S_{overexp}$
5. Δ*FGSG_10089*−FGSG_10089 C→$F_{overexp}$

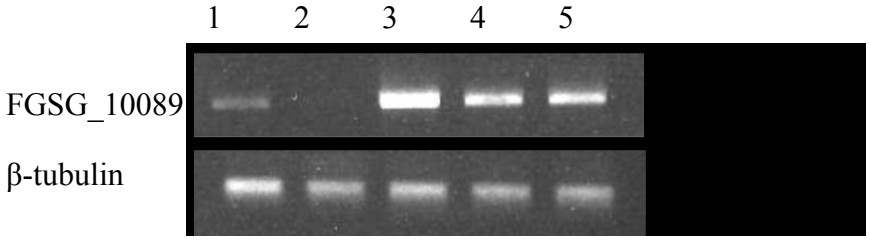

Figure 8: RT-PCR confirmation of *F. graminearum* point mutation strains

3.4 Expression patterns of *FGSG_10089* under various stress conditions

Wildtype *F. graminearum* was grown in nutrient-rich medium for 24 hours and the mycelia was then transferred into nitrogen-limiting medium. A qRT-PCR analysis was performed to examine the gene expression in nitrogen-limiting media (Figure 9). *FGSG_10089* is induced at 9 hours in this culture condition. Zero hours represents the expression after 24 hours growth in nutrient-rich media. Over time, *FGSG_10089* increased 2-fold and 5.4-fold compared to 0 hours (Figure 9). This indicated that *FGSG_10089* expression is induced by nitrogen-limiting conditions and likely has a role in virulence.

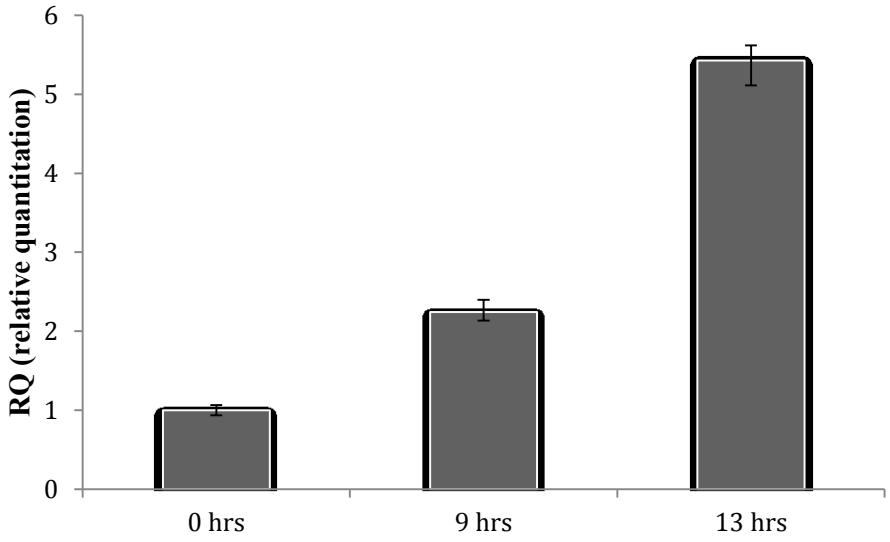

Figure 9: Expression of *FGSG_10089* is induced over time in nitrogen limiting media in WT. *FGSG_10089* expression is induced when transferred to nitrogen limiting media at 9 hours from nutrient rich media (at 0 hrs). β-tubulin is used as a control for expression levels.

Since *Tri6* is involved in virulence, we were interested to know the relationship between *FGSG_10089* and *Tri6*. As indicated in Figure 10, *FGSG_10089* expression was similar to *Tri6* at 6 hours in the nitrogen-limiting medium. However, while the expression of *Tri6* increased 2-fold and then 6-fold from 6 hours to 8 and 8 to 12 hours respectively, *FGSG_10089* expression remained constant relative to *Tri6* (Figure 10).

In addition to *Tri6*, we also monitored the expression of *FGSG_08079*. *FGSG_08079* is a regulatory gene involved in production of butenolide, another secondary metabolite production with similar kinetics as 15-ADON biosynthesis (Rampitsch *et al*., 2011). As indicated in Figure 10, the kinetics of either *Tri6* or *FGSG_08079* is not significantly affected in the Δ*FGSG_10089* strain when compared to WT (Figure 10). This suggested that any phenotype associated with the *FGSG_10089* would be independent of the two secondary metabolite pathways.

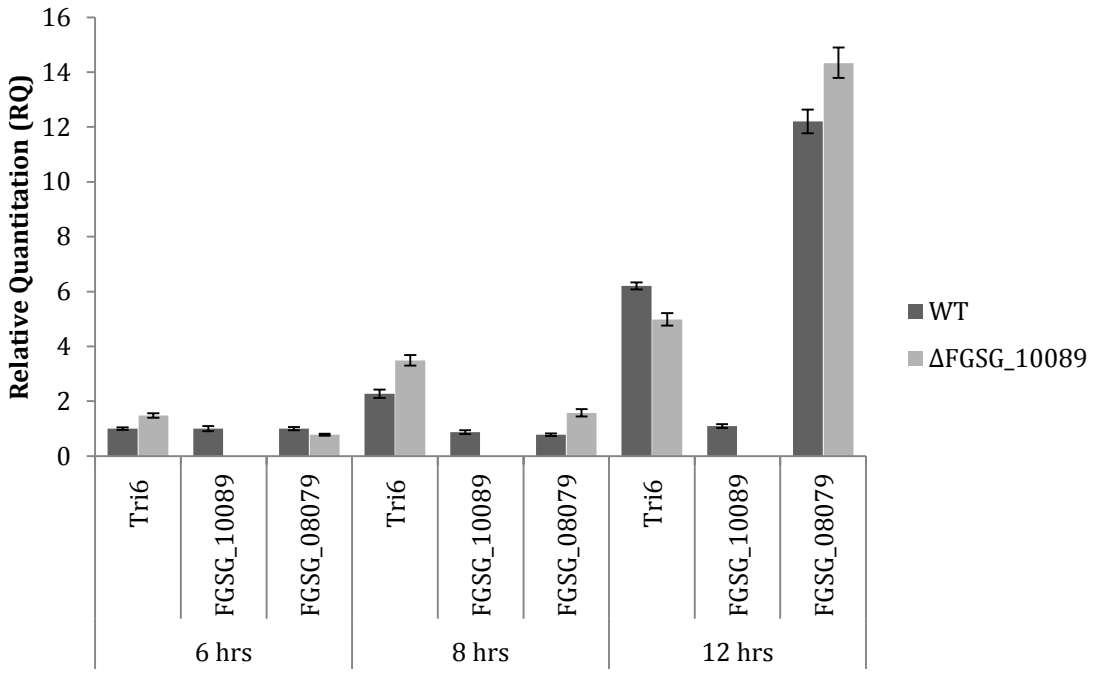

Figure 10: Expression of *Tri6* and *FGSG_08079* is not dependent on *FGSG_10089*. *FGSG_10089* expression is induced but remains constant over time. *FGSG_08079* is a marker for induction by nitrogen limiting media and is involved in butenolide synthesis.

Since *FGSG_10089* was hypothesized to be involved in sporulation, we observed its expression in sporulation inducing media, CMC (carboxymethylcellulose). Wildtype *F. graminearum* was grown in CMC for 48 and 72 hours and qRT-PCR analysis was performed on mycelia/spore production in CMC medium at these two time points (Figure 11). As the results show, *Tri6* expression was significantly up-regulated at 72 hours, compared to 48 hours; correlated with increased spore accumulation. The spore concentration was higher at 72 hours (1×10^6/ mL) compared to 48 hours (1×10^5/ mL). During this period, the expression of *FGSG_10089* remained constant (Figure 11). Even though transcript levels of *FGSG_10089* are not highly induced and remain constant under these conditions, it is possible that the protein is highly regulated at the translational or post-translational level in response to sporulation conditions.

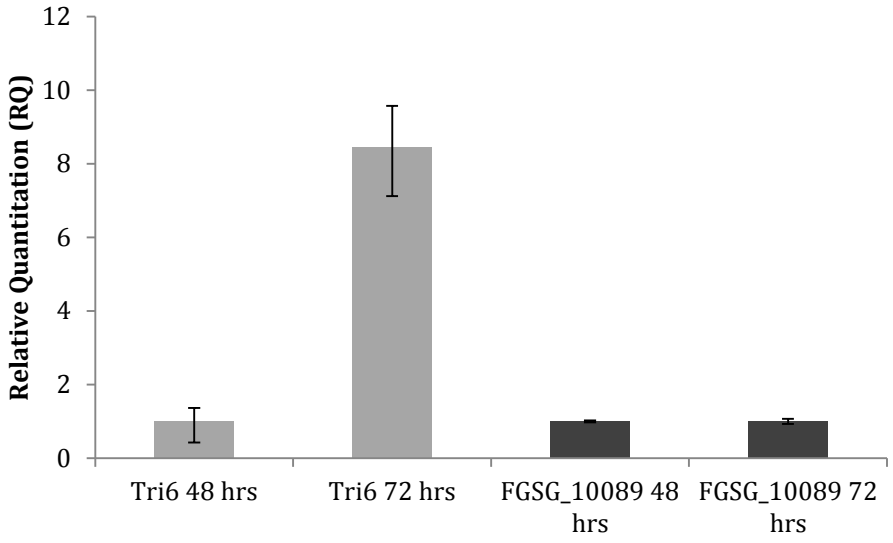

Figure 11: *FGSG_10089* is expressed but not highly up-regulated by sporulation conditions. Expression is normalized with β-tubulin and relative to expression of *Tri6* at 48 hours (hrs)

3.5 Pathogenicity is reduced in the Δ*FGSG_10089* strain

Since *FGSG_ 10089* was induced under nitrogen-limiting conditions, we assessed the virulence of Δ*FGSG_10089* strain in a pathology assay on a susceptible variety of wheat 'Roblin'. The Δ*NOXA/B* mutant has a severely reduced ability to infect wheat (Wang *et al.*, 2014). To determine if a change in FGSG_10089 activity was contributing to this phenotype, point inoculations were performed on wheat using Δ*FGSG_10089* and Δ*FGSG_10089* –FGSG_10089$_{overexp}$. The Δ*FGSG_10089* mutant was reduced in virulence on average by 43% ($P < 0.05$), compared to WT. In comparison, the *FGSG_10089* overexpressor strain (Δ*FGSG_10089*−FGSG_10089$_{overexp}$) did not show significant difference in infection (Table 2 a,c). Similar to the mutant strain, both cysteine mutant strains also displayed reduced virulence (Table 2). Mutation of cysteine residues to either serine or phenylalanine resulted in an average 38% reduction in infection ($P_{value}<0.05$) (Table 2). Overall, these results suggested *FGSG_10089* in involved in virulence and moreover, C^{325} is an important residue for functional modification of the protein and pathogenicity.

The expression of *FGSG_10089* in the Δ*FGSG_10089,* Δ*FGSG_10089* −FGSG10089$_{overexp}$, *FG10089$_{C-S}$* and *FG10089$_{C-F}$* strains were also monitored by RT-PCR analysis (Figure 8). The analysis showed that *FG10089$_{C-S}$* and *FG10089$_{C-F}$* genes were expressed at greater levels than WT (lanes 4 and 5; Figure 8).

Table 2: Pathogenicity tests of *F. graminearum* strains on wheat heads with wildtype (WT), ΔFGSG_10089, and ΔFGSG_10089 + FGSG_10089, C325S and C325F complement strains. Three independent experiments (**A** , **B** and **C**) for each strain are shown. Wheat heads were point-inoculated and scored when the WT reached >90% infected. Sample sizes represent number of wheat heads, and p-value was calculated using a two sample t-test assuming equal variances.

A

Genotype	WT	*Δfg10089-FG10089*$_{overexp}$	ΔFG10089	ΔFG10089 -*FG10089*$_{C\text{-}F\ overexp}$	ΔFG10089 -*FG10089*$_{C\text{-}S\ overexp}$
Average infected kernels (%)	**97.8 ± 1.5**	**80 ±9.2**	**54.5 ± 11.2**	**56.6 ± 10.9**	**67.9 ± 7.8**
Sample size (n)	**10**	**9**	**11**	**13**	**11**
P-value		**0.07**	**0.003**	**0.0003**	**0.02**

B

Genotype	WT	ΔFG10089	FG10089 -*FG10089*$_{C\text{-}F overexp}$	ΔFG10089 -*FG10089*$_{C\text{-}S\ overexp}$
Average infected kernels (%)	**95.1 ±3.2**	**60. 4 ±11.6**	**70. 8 ±10.5**	**67.4 ±10.7**
Sample size (n)	**10**	**10**	**12**	**10**
P-value		**0.001**	**0.05**	**0.02**

C

Genotype	WT	*Δfg10089-FG100089*$_{overexp}$	ΔFG10089	ΔFG10089 -*FG10089*$_{C\text{-}F\ overexp}$	ΔFG10089 -*FG10089*$_{C\text{-}S\ overexp}$
Average infected kernels (%)	**90.6 ±3.4**	**72.4 ±8.0**	**62.5 ±6.7**	**58.6 ±9.5**	**52 ±8.1**
Sample size (n)	**11**	**14**	**12**	**17**	**20**
P-value		**0.07**	**0.05**	**0.01**	**0.0003**

3.6 Δ*FGSG_10089* is reduced in its ability to produce 15-ADON *in vitro*

It is known that DON is an important virulence factor during infection (Gardiner *et al*., 2009). Since virulence is affected, we wanted to examine the production of 15-ADON in culture. To assess if *FGSG_10089* had a role in the 15-ADON biosynthesis pathway, we quantified 15-ADON in culture in WT and the Δ*FGSG_10089* deletion and the cysteine point mutant strains. The strains were grown for 48 hours in nitrogen-limiting medium and 15-ADON was quantified by high performance liquid chromatography (HPLC) analysis (Figure 12). The results indicated that Δ*FGSG_10089* mutant produces 14.4% less 15-ADON toxin than WT (P_{value} <0.01). Both the complemented (Δ*FGSG_10089*−FGSG10089) and the overexpressor strains (Δ*FGSG_10089*–FGSG_$10089_{overexp}$) were not significantly different from the WT in their ability to produce 15-ADON (Figure 12A). When cysteine is modified to a serine and expressed either with the native or the overexpression promoter, there is no significant difference in toxin concentration compared to WT (Figure 12A). At the end of 48 hours in the nitrogen-limiting medium, we monitored the growth of all the transgenic strains. As the results indicate, no differences were observed with respect to mycelia weight between the WT and transgenic strains (Figure 12B). Overall, the results indicate that *FGSG_10089* has a role in 15-ADON production, but unlike the pathology assays, the C^{325} does not have role in toxin production.

A

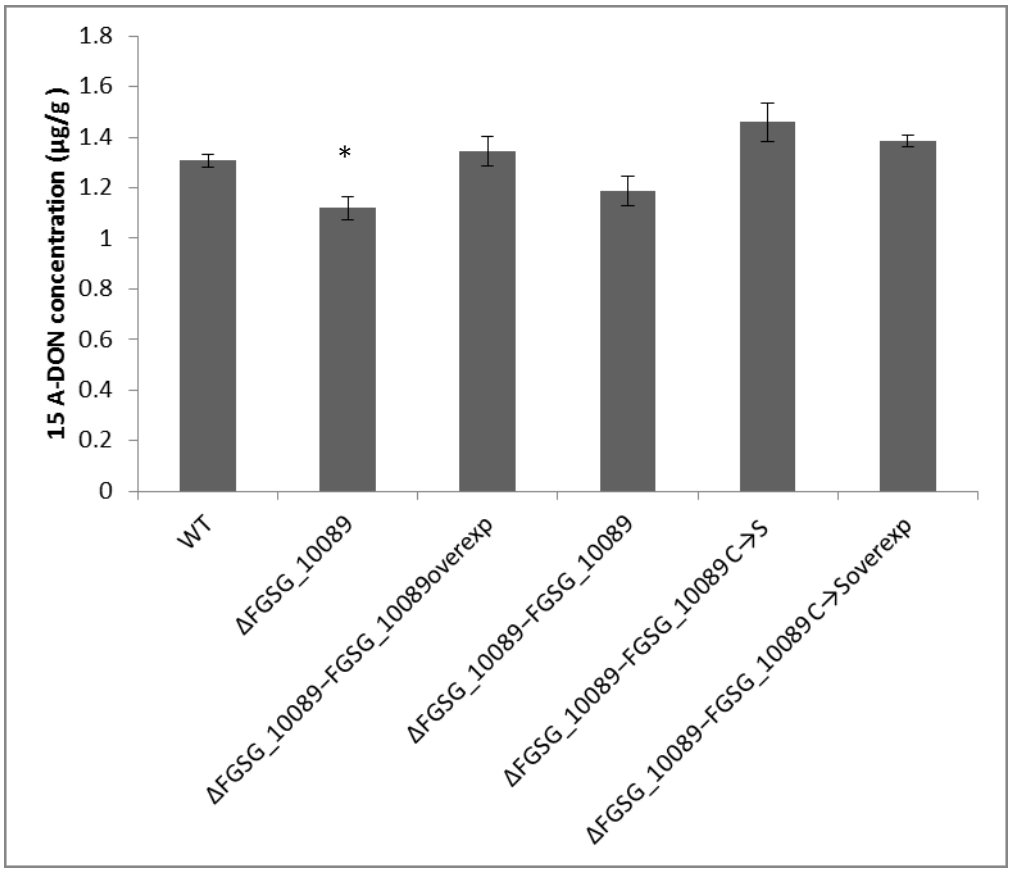

B

Sample	Average 15-ADON(ug/mg)	Average total mycelia weight (mg)
WT	**1.307**	**40.8**
ΔFGSG_10089	**1.119**	**39.5**
***ΔFGSG_10089*-FGSG_10089$_{overexp}$**	**1.345**	**40.9**
***ΔFGSG_10089*-FGSG_10089**	**1.188**	**39.8**
***ΔFGSG_10089*-FGSG_10089$_{C\rightarrow S}$**	**1.458**	**40.7**
***ΔFGSG_10089*-FGSG_10089$_{C\rightarrow Soverexp}$**	**1.383**	**39.3**

Figure 12: The *FGSG_10089* knockout produces slightly less toxin than WT (Wild-type). HPLC analysis of 15-ADON accumulation after 48 h in nitrogen-limiting media for the wildtype (WT) and the addback strains. Toxin concentration are represented based on absorbance units measured at 220 nm, in reference to a standard concentration curve for 15 A-DON, and normalized for dry mycelia weight in grams. *$p<0.0001$

3.7 Role of FGSG_10089 and cell wall integrity in *F. graminearum*

Bioinformatics analysis indicated FGSG_10089 is similar to an ECM33 (Extracellular mutant 33) (e_{val}=1x10^{-25}), a cell wall organization protein in *S. cerevisiae* with a glycosylphosphatidylinositol (GPI) anchor domain (Figure 6). ECM33 is important in sporulation and cell wall architecture in *S. cerevisiae.* Additional proteins, SPS2-Sporulation Specific 2 (YDR522c) and its paralog SPS22 are similar to ECM33 with respect to their role in in cell wall structure (Pardo *et al*, 2004; Chabane *et al*, 2006). Based on this information, we performed two experiments. First, we visualized cell wall integrity by confocal microscopy. As shown in Figure 13, when mycelia and spores were labelled with the florescent compound calcofluor white (CFW), there was no observable change in structural integrity in the Δ*FGSG_10089* strain compared to WT.

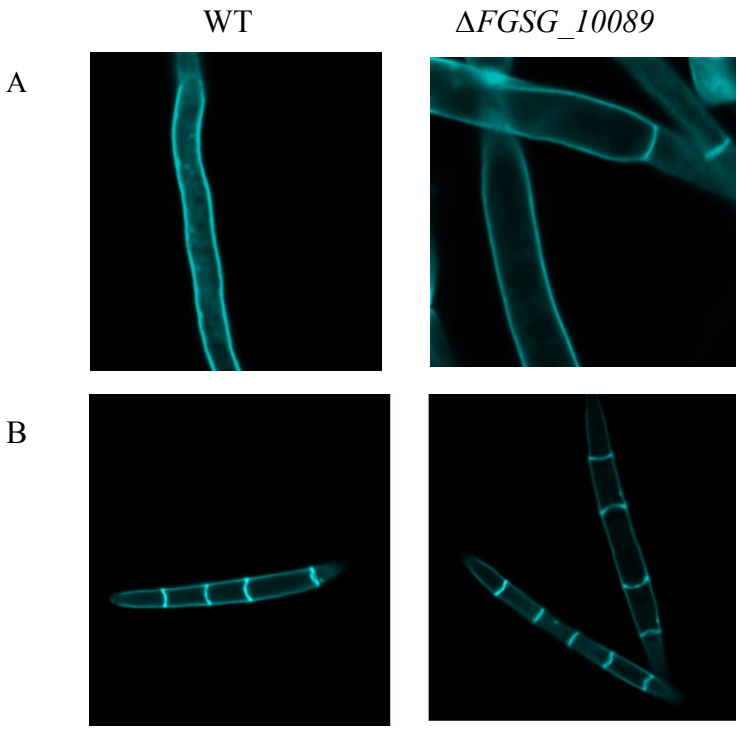

Figure 13: Structural integrity and growth of conidia and hyphae is unaltered in the Δ*FGSG_10089* mutant strain. Confocal microscopy was used to examine the cell wall structure of mycelia and conidia. Calcofluor white can be used to stain cell walls. This can be applied to A) mycelia as well as B) conidiophores

To determine if *FGSG_10089* in *F. graminearum* was functionally redundant with *ECM33*, we performed a second experiment and complemented a yeast ECM33 mutant (*ΔYBR078W*) with *FGSG_10089*. *ΔYBR078W* is sensitive to growth on CFW (Pardo *et al*., 2004). *FGSG_10089* was cloned into pYES2-DEST52 that allowed conditional expression under a galactose-inducible promoter. Empty pDEST52 vector (EV) transformed into *ΔYBR078W* was used as a negative control. After induction with galactose, Western blot confirmed that FGSG_10089 protein accumulated in yeast to high levels at 24 hours (Figure 14A). Post-induction, the cells are diluted to OD_{600}=0.5 and 5µl of a serial dilution was plated on CFW galactose YPD plates. After 4 days on 50 µg/ml CFW, we observed that FGSG_10089 was unable to rescue the growth defect seen in *ΔYBR078W* (Figure 14B). However, on 75 µg/ml CFW, there was a qualitative difference between the *YBR078W* +FGSG_10089 and the YBR078W + EV, indicating a partial complementation.

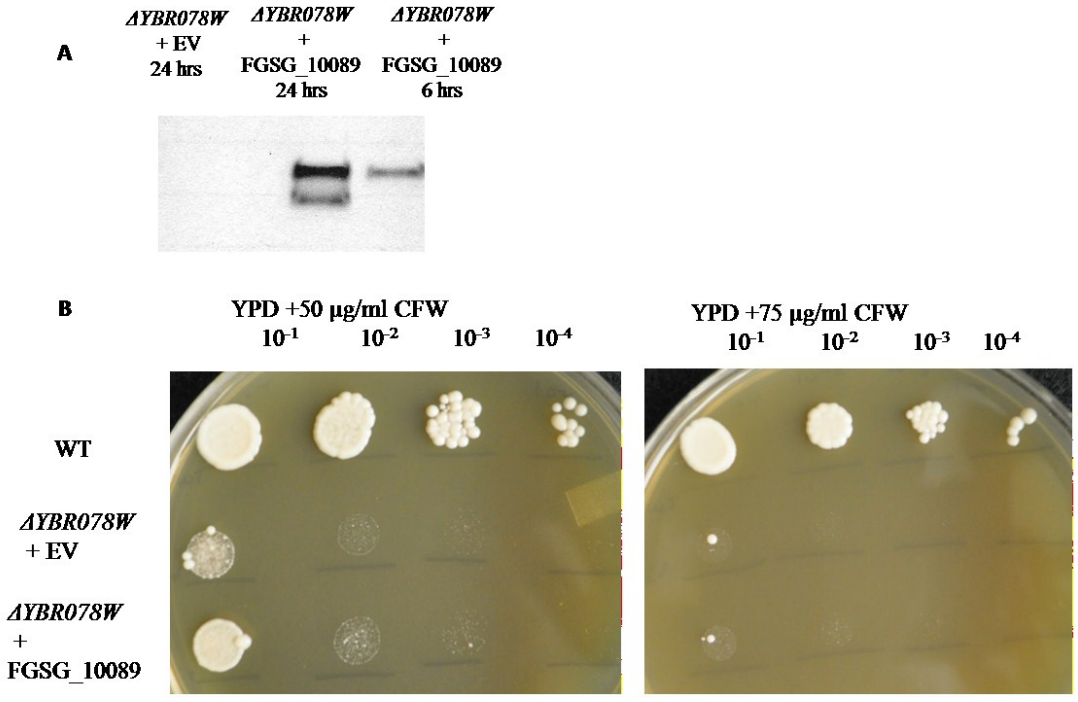

Figure 14: The Fusarium protein FGSG_10089 is unable to fully functionally complement the ECM33 null mutant. (A) FGSG_10089 is under the control of the galactose inducible promoter in the yeast Pdest52 vector. His-FGSG_10089 was detected at ~56 kDa using Histidine (C- term) Tag (6XHis) - HRP Mouse Monoclonal Antibody (R93125). (B) ΔYBR078W exhibits normal WT growth on YPD media. After 24 hours of induction in 2% YP-gal, a dilution series is plated on CFW-YPD-2% galactose plates. Plates were incubated at 28° C for 4 days

3.8 FGSG_10089 does not affect circadian rhythm

FGSG_10089 also showed homology to the *Neurospora* gene, CCG-15, which is described as having a low-amplitude rhythmic expression in mycelial culture during constant darkness after exposure to light for a certain period (Zhu *et al*., 2001). Δ*FGSG_10089* was examined for its ability to grow in a 12 hour day/light cycle. In WT, distinct bands of increased and decreased mycelial growth occur as regular circular zones. This pattern remained unaltered in Δ*FGSG_10089* (Figure 15). The increased aerial mycelial growth in the *NOXA/B* mutant obscured the circular zones (Figure 15). These results indicate that Δ*FGSG_10089* is not impaired it in its ability to respond to circadian inputs.

Figure 15: Diurnal zonation is not altered in *ΔFGSG_10089* under the conditions of 12 hours light/ 12 hrs dark for 5 days on carrot agar media. An increase in aerial mycelia is seen in *ΔFGSG_10089*. Furthermore ΔNOXA/B does not display the periodic zonation.

Chapter 4- Discussion

4.1 Overview

The most important enzymatic ROS generating system is the NADPH-dependent oxidase complex (NOX) (Heller *et al*., 2011). In filamentous fungi, the two classical protein families, enzymes NOXA and NOXB exist and by analyzing the phenotype of the corresponding mutants, diverse roles of NOX have been identified. Various studies have outlined the role of NOX in development and pathogenicity; however targets that relay these signals have yet to be identified. One way that ROS modifies its targets is through oxidation of functional groups. In particular, cysteine residues are highly conserved and can play crucial roles in the structure and function of proteins. They can act as "redox sensors" in the cell and transduce structural changes to functional changes in the protein upon formation of a disulfide bond (McDonagh *et al*., 2009). In this study, we focused on the oxidation of the cysteine thiol group in the *F. graminearum* proteome in the *ΔNOXA/B* double mutant compared to wildtype.

4.2 Redox proteomics to identify differentially oxidized targets

Redox modifications that were not examined include reactions with small molecular weight thiols such as glutathione (GSH), which creates an intermolecular disulfide (Figure 16). Additional oxidative modifications include cysteine-nitrosylation, tyrosine nitration and carbonylation. Tyrosine nitration occurs when cysteine on the protein reacts with peroxynitrite or nitrosothiols (Ghezzi *et al*., 2003). Carbonylation is often referred to as "oxidative damage," which is indicative of a modification that implies oxidative stress rather than redox regulation (Ghezzi *et al*., 2003). Protein carbonyls

result from ROS reacting with side chains of one of several amino acids (lysine, arginine, proline, and threonine) (Ghezzi *et al*., 2003).

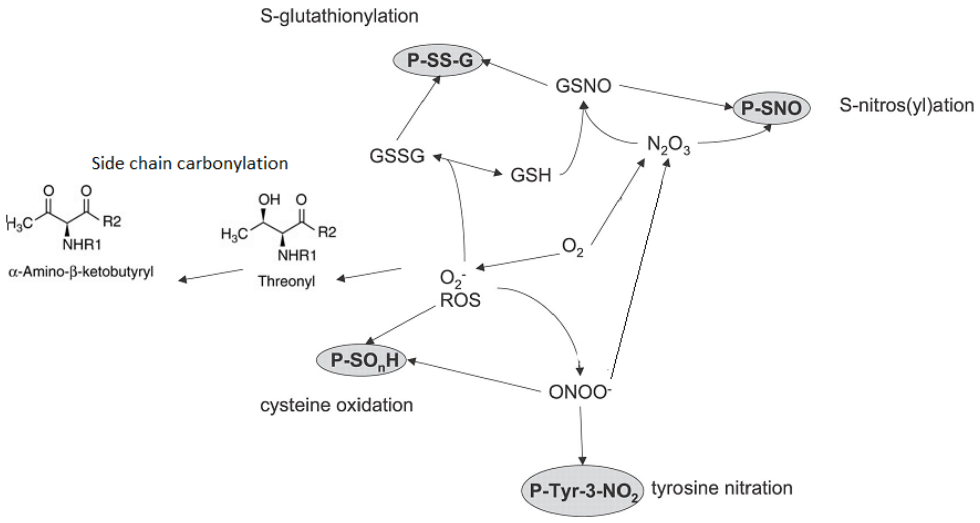

Figure 16: Chemical relationship among different reactive oxygen species (ROS) and reactive nitrogen species (RNS), and their impact on some post-translational modification of proteins. Modified from Martínez-Lopez *et al*., 2004 Copyright © 2004, European Society of Cardiology

In order to identify differentially oxidized cysteine targets, a gel-free proteomics was employed. Gel-free proteomics overcomes some other limitations incurred by gel-based methods. When looking at entire cell/tissue extracts, gel-free methods have increased sensitivity allowing for the detection of low abundance proteins (Baggerman *et al*., 2005). Also, proteins that are difficult to separate because of their inherent physiochemical properties such as PI, molecular weight and hydrophobicity (membrane proteins) are more easily separated (Baggerman *et al*., 2005). These advantages are conferred by the use of high-performance liquid chromatography (HPLC) coupled to a mass spectrometer, which is preceded by enzymatic digestion of the entire protein extract (Baggerman *et al*., 2005). Since this is interfaced with a powerful triple quadrupole time of flight (Q-TOF) mass analyzer, an accurate detection of the relative abundance ratio of peptides in such a complex sample can be completed with high certainty (Yates *et al*., 2009). One other key advantage is the ability to label peptides prior to analysis, which in this case confers the specificity of only retaining cysteine disulfide modifications.

Using this method, we identified 16 targets of NOX generated ROS in *F. graminearum* under nitrogen limiting conditions. Of these targets, a large proportion was involved in metabolism. While there has been no published assessment of proteins affected by NOX, a study in *Saccharomyces cerevisiae* looked at the thiolic "redox proteome" using a gel-free method following addition of H_2O_2. This study found a significant impact upon metabolism, including the glycolytic enzymes such as fructose bisphosphate aldolase which has also been identified in other related studies as being

sensitive to oxidation (McDonagh *et al*., 2009; Di Domenico *et al*., 2010; Brandes *et al*., 2011). Another study in the same organism identified enolase and pyruvate decarboxylase, which are present in our study and are subject to oxidative modification (Cabiscol *et al*., 2000; Shenton *et al*., 2003). Other proteins with similar function that were in common with our study were also identified. These included cell wall proteins such as 1,3-betaglucanosyl transferase and an uncharacterized GPI-anchored cell wall protein (Shenton *et al*., 2003). Thus overlap of gene categories with other studies supports the method for redox sensitive cysteine residue identification within the proteome. We observed that oxidation is reduced in the cysteine residues of all the proteins at some point during the time course (Table 1). All 16 potential NOX targets show a significant change in trend in the oxidation status between the knockout and WT strains, suggesting that proteins might undergo change in activity. An example of oxidation that causes a decrease in activity of an enzyme is the human protein tyrosine phosphatase PTP1B, where a thiol in the active site was modified by H_2O_2 (Apel and Hirt, 2004).

4.3 ROS plays important role in cellular signal transduction

From the 16 proteins, we focused on the role of one, specifically FGSG_10089 which is a putative secreted cell wall protein with a glycosylphosphatidylinositol (GPI) anchor. FGSG_10089 is less oxidized at 6 hours in Δ*NOXA/B* than in WT. If the C^{325} is involved in an intermolecular disulfide, loss of this oxidation induced linkage could affect essential protein interactions and its function. This change is reflected in the loss of pathogenicity seen in both the *FGSG_10089* knockout and point mutation strains,

indicating that the structure conferred by C^{325} is critical for the role of FGSG_10089 in interacting with the host.

Characterization of the role of cysteine residues in fungal GPI anchor proteins is limited. An example of the importance of disulfide bonds in protein structure come from a protein characterized in *Escherichia coli* (Jo *et al*., 2015). The OxyR transcription factor is active only under oxidized conditions to create a disulfide bridge, which changes its conformation, required for DNA binding (Jo *et al*., 2015). Another example comes from mammalian studies of the GPI-anchor protein, Thy-1 cell surface antigen (also thymocyte differentiation antigen-1) of the immunoglobulin superfamily. Loss of oxidation leads to loss of epitope recognition by these antibodies (Bradley *et al*., 2013). In our study, the observed change in pathogenicity of Δ*FGSG_10089* mutant and point mutation strains is likely due to a structural change in the cell wall or a change in the ability of FGSG_10089 to interact with other proteins involved in cell wall architecture.

4.4 FGSG_10089- A structural analysis

While the function of FGSG_10089 has yet to be elucidated, its function can be inferred from structural analysis of other proteins with similar motifs. FGSG_10089 is similar to ECM33 (Extracellular mutant 33), a cell wall organization protein with a GPI anchor in *S. cerevisiae*. Covalent attachment of the GPI allows a protein to be anchored to the cell wall (Figure 17). In a GPI anchor, the phosphatidylinositide group is connected to a sugar chain that ends with the terminal phosphoethanolamine (PE) residue. The amino group of the (PE) moiety is used to attach the GPI anchor to the C terminus of the target protein (Rittenour *et al*., 2013; Vishwakarma *et al*., 2005) (Figure 17).

GPI anchors can be predicted using bioinformatics tools since they contain conserved regions, including an N-terminal signal peptide and C-terminus anchor (Eisenhaber, 2004). In addition to these components there are 3 critical structural motifs that can be used to predict the likelihood that the protein is a GPI anchor protein, with 90% accuracy. These regions include the site at the C-terminus where the GPI moiety is attached (ω-site), (ii) a moderately polar spacer region and a hydrophobic C-terminal region which is also about 10–20 residues and subsequently cleaved off upon attachment of the GPI in the ER (deGroot *et al*., 2003) (Eisenhaber *et al*., 1998). All of these canonical signatures exist in FGSG_10089, which leads to its high score from the fungal GPI anchor prediction algorithm.

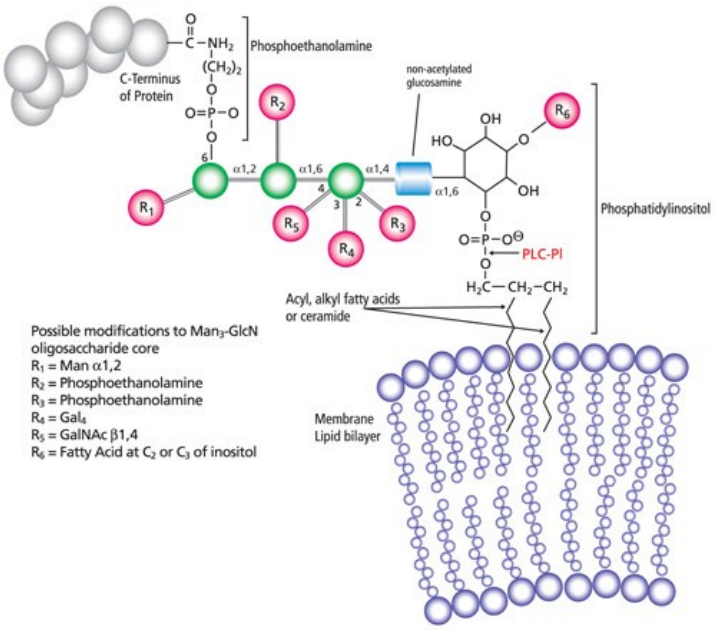

Figure 17: The composition of a glycosylphosphatidylinisotol (GPI) anchored protein at the membrane.

In addition to the GPI-anchor and cysteine residues, bioinformatics analysis revealed that FGSG_10089 also contains a putative L-domain as well as an LRR (leucine rich repeat) domain. The L-domain typically contains 10-16 % leucine, similar to the leucine content (17%) of the L-domain in FGSG_10089 (Ward *et al*., 2001). The L-domain (IPR000494) consists of a single-stranded right-handed beta-helix, and is known to bind ligands, such as the epidermal growth factor receptor (EGFR) family members, involved in cell proliferation, differentiation and apoptosis (Schmiedel *et al*., 2008; Ward *et al*., 2001). The only other fungal protein that this domain has been identified in is the ECM33 protein in yeast (Pardo *et al*., 2004). The capacity and purpose for this protein to bind ligands in fungi however has not been studied.

Recently, ECM33 from yeast and several other fungi have also been described to contain a newly discovered non-canonical LRR (leucine rich repeat) domain called the IRREKO sequence (Miyashita *et al*., 2014a). The authors propose that the non-canonical LRR domain in ECM33 contributes to interactions with unknown targets to achieve the functions described above (Miyashita *et al*., 2014a). Previous to this study canonical LRR proteins were not found to exist within the fungi Kingdom (Soanes and Talbot, 2010). These domains are involved in protein-ligand or protein-protein interactions, where the LRR domain confers recognition specificity during the plant or human-immune response during interaction with a pathogen (Baker *et al.,* 1997). Since FGSG_10089 contributes to the pathogenicity response, it may function as a recognition factor that the plant senses in order to mount a defense response against the fungus.

4.5 Role of GPI-anchor proteins

Studies have shown that in yeast, ECM33 is required for proper yeast spore formation. Deletion of *ECM33* in *S. cerevisiae* results in the loss of cell wall integrity and defects in glycosylation pathway (Pardo *et al*., 2004). In fungi, GPI-anchor proteins such as ECM33 localize at the cell wall where they can then be covalently attached. They have a broad range of function and have been shown to act as adhesins and in cell wall biosynthesis (Mouyna *et al*., 2000; Guo *et al*., 2000). In the human pathogenic fungi *Candida albicans*, ECM33 is associated with antigenicity responses and virulence (Martinez-Lopez, 2004). In the ascomycete *Magnaporthe grisea*, mutation of a GPI-anchor protein, *EMP1* exhibited reduced levels of appressorium formation and pathogenicity, which was attributed to a loss of cell wall (Ahn, 2004).

In contrast, in *Fusarium* the contribution of cell wall and secreted proteins to virulence is not well characterized. In a study by Rittenour *et al* (2013) they found that out of the ~14,000 encoded proteins in *F. gramineraum*, 205 were predicted to have a GPI-anchor signal. In the global search to ascertain functions for GPI anchor proteins, they discovered various predicted functions associated with GPI-anchor proteins, including cutinases, aspartyl proteases, and proteins with the conserved cysteine-rich fungal extracellular membrane (CFEM) domains. Collective functions of these proteins indicate their role in pathogenicity. Characterization of one GPI anchor protein, GPI7 in *Fusarium*, showed a subtle effect on composition of the cell wall (Rittenour *et al*., 2013). Moreover, a *gpi7* mutant had reduced growth rate and infection on wheat heads.

4.6 Characterizing the role of FGSG_10089 in the cell

Several large scale genomic and proteomics studies in several environmental conditions in *F. graminearum* have identified FGSG_10089 as being expressed and secreted (Phalip *et al*., 2005; Yang *et al*., 2012; Ji *et al*., 2013). Proteomics analysis of secreted proteins of *F. graminearum* grown in medium containing cell wall derived from hops plants identified FGSG_10089 (Phalip *et al*., 2005). To mimic the nutritional situation in-planta, another study grew *F. graminearum* on wheat or barley flour media and the secreted proteins were separated by two-dimensional gel-electrophoresis, also identified FGSG_10089 (Yang *et al*., 2011). A third, more recent study used shot-gun proteomics in an effort to detect new putative virulence factors. They grew *Fusarium* on minimal media lacking organic nitrogen and also found that FGSG_10089 is secreted (Ji *et al*., 2013). This is consistent with the presence of a secreted signal identified by bioinformatics analysis.

Interestingly, infection of *Fusarium* by a *Fusarium*-specific virus, DK21, also identified a significant change in accumulation of FGSG_08737, FGSG_06932, FGSG_01346, FGSG_04826, FGSG_09321; all of which are found in our NOX redox proteome (Kwon *et al*., 2009). A role for these NOX substrates during fungus-virus interaction is not known, but it underscores the importance the role that NOX might play in various interactions.

In support of our hypothesis that FGSG_10089 functions as a virulence factor, we performed experiments to observe its expression in various environmental conditions,

conducive for the production of virulence factors. We observed that *FGSG_10089* expression is induced under nitrogen-limiting conditions, similar to *Tri6* at 6 hours and the expression is maintained for the next 24 hrs. Since this protein contributes to infection, it is reasonable that it is also induced under such conditions. This is validated by the observation that 99% of transcripts that were found in trichothecene inducing conditions (nitrogen limiting) were also found to be expressed during infection conditions *in-planta* (Taylor *et al*., 2008). Expression of *Tri6* in Δ*FGSG_10089* is not significantly different compared to WT, which suggested that *FGSG_10089* does not have an effect on the production of 15-ADON through the global regulator, Tri6.

ECM33 is part of the SPS2 (sporulation specific) family that has shown to be important for cell wall formation in yeast and we expected that *FGSG_10089* may also be expressed during conditions of sporulation (Pardo *et al*., 2004). In this study, it was found that *FGSG_10089* is in fact expressed under stress conditions by growth in CMC. In a study where an Affymetrix Genechip platform was used to monitor gene expression in *Fusarium* during specific stages of conidial germination, it was discovered that many significantly up-regulated genes belonged to the oxidative stress response (Seong *et al*., 2008). *FGSG_10089*, was one of the ~7% of genes that were upregulated between 8 and 24 hours, when hyphae from germinated conidia expand and laterally branch (Seong *et al*., 2008).

Our results showed that modification of the C^{325} to a serine or phenylalanine resulted in decreased virulence function of the FGSG_10089 protein. Pathology tests on

wheat revealed that similar to the *FGSG_10089* knockout strain, there was an average infection of 62% for both point mutants. From this data it is apparent that the C^{325} residue that is oxidized in FGSG_10089 is essential for the protein's role in pathogenicity. It is also possible that the mutation may have a general effect on protein function due to its inability to form a disulfide bridge. Exactly, how the cysteine contributes to folding of the protein cannot be assessed with high certainty *in-silico* as there is no close homolog for this domain for which a crystal structure has been obtained. Although, virulence is affected, biosynthesis of 15-ADON is not affected by the point mutants. This suggests that, within the FGSG_10089 protein, there are domains responsible for various functions, including virulence and a capacity to interact with signaling pathways involved in mycotoxin production.

4.6.1 FGSG_10089 does not fully complement the yeast *ΔYBR078w* (ECM33) mutant

To further understand the role of FGSG_10089 in the cell, a complementation assay was conducted. The expression of FGSG_10089 protein within the *ecm33* knockout was not able to dramatically revert the susceptibility of the *ΔYBR078w* mutant to calcofluor white (CFW). CFW has a high affinity for cellulose and chitin in the cell wall. As a consequence, the assembly of microfibril in the cell wall is severely impaired. In cells that have a pronounced disorganization of the cell wall, CFW can more readily permeate and bind, which creates the sensitivity phenotype (Roncero, 1985). There are several reasons for the lack of complementation of the mutant by FGSG_10089. First, it is possible that the *Fusarium* GPI- anchor has evolved a different function other than cell wall organization. This is supported by the observation of another GPI-anchor protein

GAS1, which was also unable to complement its yeast paralog (Caracuel, 2005). Lack of complementation was attributed to either sequence divergence or lack of relevant post-translational processing in yeast (Caracuel *et al*., 2005).

4.6.2 Contribution of other putative targets of NOX to *F. graminearum* pathogenicity

Among the 16 proteins that were identified as targets of NOX, deletion of *FGSG_08737* also resulted in a reduction of *Fusarium* infection on wheat after point inoculation. This gene encodes for a woronin body protein, which functions in an emergency response when there is damage to hyphae (Markham *et al*., 1987). They prevent hyphal damage by blocking the area in septal pores to prevent excessive cytoplasm leakage, which would eventually cause hyphal rupture and cell death (Markham *et al*., 1987). During the infection process, plants secrete degradative enzymes and ROS. Thus, an inability to protect damaged mycelia would affect infection ability of the fungi. It would be interesting to characterize this in the *FGSG_08737* mutant strain.

Another target of NOX found in this study is FGSG_02022, which is also a GPI-anchor protein. We were unable to obtain a knockout for this gene in *F. graminearum*. *FGSG_02022* encodes for a β1,3 glucanosyltransferase and is known in other systems to be involved in cell wall biosynthesis and morphogenesis (Popolo *et al*.,1993). In *Fusarium oxysporum,* it was demonstrated that a loss of function of this protein resulted in dramatically reduced virulence on tomato plants (Caracuel *et al*., 2005). It was proposed that this change in virulence could be attributed to a loss of recognition of the host surface by the pathogen. Since the mutant showed a defect in hyphae

morphogenesis, an essential structure for invading a host, it was proposed that lack of disease by this mutant is due to its inability to penetrate the host cell wall (Caracuel *et al*., 2005).

4.7 FGSG_10089 is part of a virulence network

Relationships including protein similarity, co-regulation, predicted interactions and co-expression allow us to decipher the function of a protein. Thus a network based approach was undertaken in *Fusarium* where FGSG_02022 was predicted to be a virulence associated protein (Lysenko, 2013). In addition, *FGSG_08737* is one of the genes identified in the network analysis as a virulence factor. This study supports our hypothesis that *FGSG_08737* is required for pathogenicity upon infection of wheat (Son *et al*., 2013).

A transcriptome analysis of Δ*NOXA/B* and *Δtri6* mutant in nutrient-rich conditions showed that the expression of *FGSG_10089* changed in the two mutant backgrounds (Subramaniam, unpublished). It was found that the expression of *FGSG_10089* was 4-fold higher in the WT compared to the Δ*NOXA/B* mutant. In comparison with the *Δtri6* mutant, the expression of *FGSG_10089* was 2-fold higher in the WT *F. graminearum*. Interestingly, the expression of *FGSG_02022* was similarly regulated by the two mutants. There was a 6-fold higher expression in the WT than Δ*NOXA/B* and 2-fold higher in WT than *Δtri6.* Based on these data, co-expression of the two GPI-anchor proteins, regulated by both *NOXA/B* and *Tri6* supports the notion that there is an intersection between these two pathways.

4.8 Network analysis reveals genetic links between signaling pathways

Network analysis in *Saccharomyces cerevisiae* shows a genetic link (green lines) and physical link (pink lines) between NOXA (yeast orthologue AIM14) and FGSG_10089 (similar yeast protein ECM33) (Figure 18). Analysis also show that ECM33 is connected to various cell wall components. This is expected since in yeast ECM33 contributes to cell wall integrity. For example, one genetic interaction occurs with *Mcd4* which is involved in glycosylphosphatidylinositol synthesis (Wiedman *et al*., 2007). Another genetic interaction occurs with *Las21,* an integral plasma membrane protein which contributes to the formation of GPI anchors. A mutation in this gene affects cell wall integrity (Benachour *et al*., 1999). It physically interacts with YGP1, a secreted glycoprotein at the cell wall, which is induced by nutrient deprivation-associated growth arrest (Destruelle *et al*., 1994). The strength of genetic interaction between *Ecm33* and *Pst1* stems from the study that showed an exacerbation of the *Δecm33* phenotype (Pardo *et al*., 2004). Based on this, it would be interesting to see if FGSG_10089 also displays an increased loss of pathogenicity when deleted with another cell wall component.

Furthermore, *Ecm33* genetically interact with *Aim14* through *Act1*, which encodes for actin, a major cytoskeletal filament that is involved in cell polarization. Since the knockout of *Aim14* has a phenotype of delocalized chitin deposition and abnormal cell shape, it is reasonable that it genetically interacts with *Ecm33*, which also effects the cell wall composition (Botstein *et al*., 1997). In addition, it is recorded that AIM14 is involved in superoxide mediated regulation of the actin skeleton (Rinnerthaler *et al*., 2012). Lastly, *Aim14* is linked to *Slt2,* and thus Ecm33 through MCA1, which is a cysteine protease involved in the stress response and apoptosis after treatment with H_20_2

(Madeo *et al*., 2002). Since AIM14 is involved in both cell wall integrity and the stress response, it is reasonable that it is connected to both SLT2 and ECM33. This is supported by a study which observed that the phenotype of increased apoptosis by overexpression of *Aim14* was suppressed by a *mca1* null mutation (Rinnerthaler *et al*., 2012). In *Fusarium*, the interaction of NOX with these components has not been identified.

In this network, we observe that ECM33 has a genetic interaction with SLT2, the homolog to *Fusarium* Mgv1, a MAP kinase that is involved in maintenance of cell wall integrity, sexual reproduction and the production of mycotoxin (Hou, 2002). Genetic interaction implies that the two genes are part of parallel genetic pathways that contributes to a phenotype. It is possible that FGSG_10089 is interacting with components in the cell wall that are also targets of the MAP kinase and the NOX pathway. Since, both NOX and MAP kinase pathways contribute to virulence; network analysis may identify previously uncharacterized proteins as part of the virulence network in *F. graminearum.*

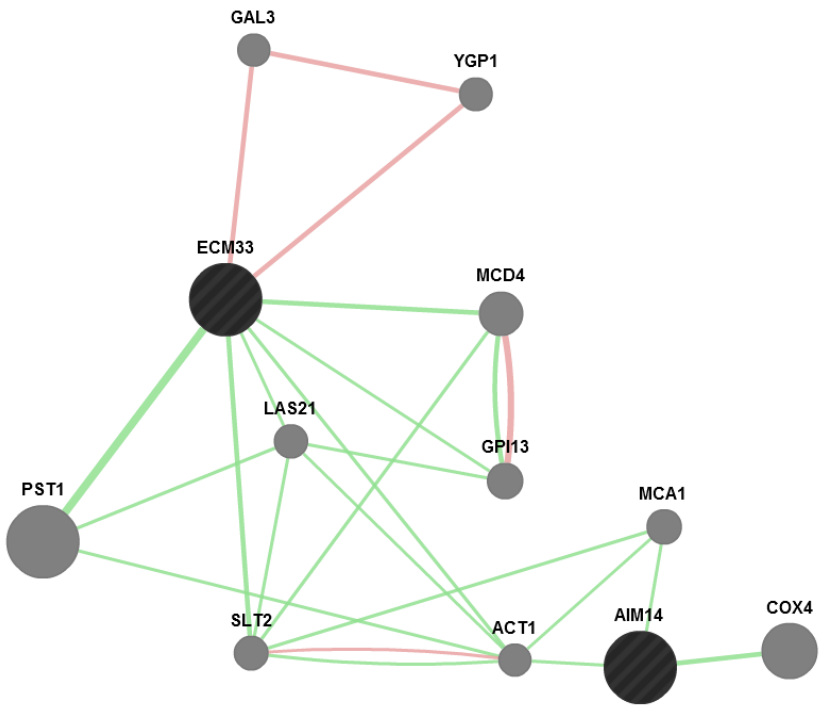

Figure 18: Network analysis in *Saccharomyces cerevisiae* using the "GeneMANIA" web program using Aim14 and ECM33 as the input.

Appendix:

Appendix Table 1: Primers used in standard PCR and qRT-PCR reactions for the generation of transgenic constructs and verification of construct integration

Generate TOPO clone	
Fg 10089 Entr F	caccATGCATTCCGTTAAGGTTC
Fg 10089 Entr R	GAAGATCTGAGCGAGAGCAGC
Overexpression clone (prF-GUE)	
Forward User 10089_His	GGACTTAAUATGCATTCCGTTAAGGTTC
Reverse User 10089_His	GGGTTTAAUAGCGGGTTTAAACTCAATG
FG_10089 FWD	GACCTTGTCAACATCACC
FG10089_Seq4_REV	CTTCTCGAAGCTACCACGG
Primers used for point mutations	
Fg 10089 int MF	GAGGAGTTCTTCAAATACTTTG
Fg 10089 int MR	CAAAGTATTTGAAGAACTCCTC
Fg 10089 int1 MF	GAGGAGTTCTCCAAATACTTTG
Fg 10089 int1 MR	CAAAGTATTTGGAGAACTCCTC
Primers to confirm FGSG_10089 deletion/presence	
Fg 10089 seq F	GACCTTGTCAACATCACC
FG10089 Seq4 R	CTTCTCGAAGCTACCACGG
10089 cds_FWD	ACTCGGTATCTCTGCCGTCT
10089 cds_REV	CACTTCTCCTCGCCGTCAAT
Gen F	GAAGCACTTGTCCAGGGAC
Gen R	GACCGACCTGTCCGGTGCCC
Primers for complement strain	
Fwd1_FG10089user_promoter	GGACTTAAUAGCCGAAACTGACCTGTTGG
Rev1_FG10089promoter_cds_user	CTTAACGGAATGCATTATGACCTG
FWD2_FG10089cds	ATGCATTCCGTTAAGGTTCTTAAG
REV2_FG10089cds_user	GGGTTTAAUTTAGAAGATCTGAGCGAGAGCAGC
REV3_FG10089cds_user	GGGTTTAAUTTAGAAGATCTGAGCGAG
RT/qRT-PCR primers	
Qpcr10089FWD1:	CGACCTGAAGAAGGACAAGAAG
Qpcr10089REV1	TGCTTTGGGAAGAACCAGAG
FWD1_10089RTPCR	CCCCCTGCTTGAGGAGATTG
REV1_10089RTPCR	AAGATCTGAGCGAGAGCAGC

References

Aguirre, J., Rios-Momberg, M., Hewitt, D., & Hansberg, W. (2005). Reactive oxygen species and development in microbial eukaryotes. *Trends Microbiol*. 13, 111–118.

Ahn, N., Kim, S., Choi, W., Im, K-H, & Lee, Y-H. (2004). Extracellular matrix protein gene, *EMP1*, is required for appressorium formation and pathogenicity of the rice blast fungus, *Magnaporthe grisea*. *Mol Cells*. 17, 166-173.

Alexander, N.J., McCormick, S.P., Waalwijk, C., Van der Lee, T., & Proctor, R.H. (2011). The genetic basis for 3-ADON and 15-ADON trichothecene chemotypes in Fusarium. *Fungal Genet Biol*. 48, 485–495.

Amberg, D. C., Burke, D. J., & Strathern, J. N. (2005). Methods in Yeast Genetics: A Cold Spring Harbor Laboratory Course Manual, 2005 Edition (Cold Spring).

Apel, K., & Hirt, H. (2004). Reactive oxygen species: metabolism, oxidative stress, and signal transduction. *Annu. Rev. Plant Biol*. 55, 373-399.

Baggerman, G., Vierstraete, E., De Loof, A., & Schoofs, L. (2005). Gel-based versus gel-free proteomics: a review. *Combinatorial chemistry & high throughput screening*. *8*(8), 669-677.

Bai, G., & Shaner, G. (2004). Management and resistance in wheat and barley to Fusarium head blight 1. *Annu. Rev. Phytopathol.*, 42, 135-161.

Baker, B., Zambryski, P., Staskawicz, B., & Dinesh-Kumar, S. P. (1997). Signaling in plant-microbe interactions. *Science*. 276(5313), 726-733.

Barbosa, .I.P., & Kemmelmeier, C. (1993).Chemical composition of the hyphal wall from *Fusarium graminearum*. *Exp Mycol.* 17, 274-283. .

Bayram, Ö., Krappmann, S., Ni, M., Bok, J. W., Helmstaedt, K., Valerius, O., *et al*. (2008). VelB/VeA/LaeA complex coordinates light signal with fungal development and secondary metabolism. *Science*. 320(5882), 1504-1506.

Bayram, O. S., Bayram, Ö., Valerius, O., Park, H. S., Irniger, S., Gerke, J., *et al*. (2010). LaeA control of velvet family regulatory proteins for light-dependent development and fungal cell-type specificity. *PLoS Genet*. 6(12), e1001226-e1001226.

Benachour, A., *et al*. (1999). Deletion of GPI7, a yeast gene required for addition of a side chain to the glycosylphosphatidylinositol (GPI) core structure, affects GPI protein transport, remodeling, and cell wall integrity. *J Biol Chem.,* 274(21), 15251-61.

Boenisch, M. J., & Schäfer, W. (2011). *Fusarium graminearum* forms mycotoxin producing infection structures on wheat. *BMC plant biology*. 11(1), 110.

Botstein D, *et al*. (1997). "The yeast cytoskeleton." in The Molecular and Cellular Biology of the Yeast *Saccharomyces*: Cell Cycle and Cell Biology, edited by Pringle JR, Broach JR and Jones EW. Cold Spring Harbor, NY: Cold Spring Harbor Laboratory Press.

Bradley, J. E., Chan, J. M., & Hagood, J. S. (2013). Effect of the GPI anchor of human Thy-1 on antibody recognition and function. *Laboratory Investigation*. *93*(3), 365-374.

Brandes, N., Schmitt, S., & Jakob, U. (2009). Thiol-based redox switches in eukaryotic proteins. *Antioxidants & Redox Signaling*. 11(5), 997-1014.

Brandes, N., Reichmann, D., Tienson, H., Leichert, L. I., & Jakob, U. (2011). Using quantitative redox proteomics to dissect the yeast redoxome. *Journal of Biological Chemistry*. 286(48), 41893-41903.

Breitenbach, M., Weber, M., Rinnerthaler, M., Karl, T., & Breitenbach-Koller, L. (2015). Oxidative Stress in Fungi: Its Function in Signal Transduction, Interaction with Plant Hosts, and Lignocellulose Degradation. *Biomolecules*, 5(2), 318-342.

Brown, N. A., Urban, M., Van de Meene, A. M., & Hammond-Kosack, K. E. (2010). The infection biology of *Fusarium graminearum*.Defining the pathways of spikelet to spikelet colonisation in wheat ears. *Fungal Biology*. 114(7), 555-571.

Buerstmayr, H., Ban, T., & Anderson, J.A. (2009). QTL mapping and marker-assisted selection for Fusarium head blight resistance in wheat: a review. *Plant Breeding.*128, 1–26.

Bushnell, W. R., Hazen, B. E., Pritsch, C., & Leonard, K. J. (2003). Histology and physiology of Fusarium head blight. *Fusarium head blight of wheat and barley*. USA, St. Paul. American Phytopathological Society, 44-83.

Cabiscol, E., Piulats, E., Echave, P., Herrero, E., & Ros, J. (2000). Oxidative stress promotes specific protein damage in *Saccharomyces cerevisiae*. *Journal of Biological Chemistry*. 275(35), 27393-27398.

Cappellini, R. A., & Peterson, J. L. (1965). Macroconidium formation in submerged cultures by a non-sporulating strain of *Gibberella zeae*. *Mycologia*. 962-966.

Caracuel, Z., Martínez-Rocha, A. L., Di Pietro, A., Madrid, M. P., & Roncero, M. I. G.

(2005). Fusarium oxysporum gas1 encodes a putative β-1, 3-glucanosyltransferase required for virulence on tomato plants. *Molecular Plant-Microbe Interactions*. 18(11), 1140-1147.

Chabane, S., Sarfati, J., Ibrahim-Granet, O., Du, C., Schmidt, C., Mouyna, I., *et al*. (2006). Glycosylphosphatidylinositol-anchored Ecm33p influences conidial cell wall biosynthesis in *Aspergillus fumigatus*. *Applied and Environmental Microbiology*. 72(5), 3259-3267.

Chen, Y., Zhu, J., Ying, S. H., & Feng, M. G. (2014). The GPI-anchored protein Ecm33 is vital for conidiation, cell wall integrity, and multi-stress tolerance of two filamentous entomopathogens but not for virulence. *Applied Microbiology and Biotechnology*. 98(12), 5517-5529.

Cuomo, C., Güldener, U., Xu, J.R., Trail, F., Turgeon, B.G., Di Pietro, A., *et al*. (2007). The Fusarium graminearum genome reveals a link between localized polymorphism and pathogen specialization. *Science.* 317**:** 1400–1402.

Deacon J.W. (2006). *Fungal Biology*, Ed 2. Blackwell Publishing, Malden, MA, 204–206.

De Groot, P. W., Hellingwerf, K. J., & Klis, F. M. (2003). Genome-wide identification of fungal GPI proteins. *Yeast*. 20(9), 781-796.

Delaunay, A., Isnard, A. D., & Toledano, M. B. (2000). H2O2 sensing through oxidation of the *Yap1* transcription factor. *The EMBO Journal*. 19(19), 5157-5166.

Destruelle M, *et al*. (1994). Identification and characterization of a novel yeast gene: the YGP1 gene product is a highly glycosylated secreted protein that is synthesized in response to nutrient limitation. *Mol Cell Biol,* 14(4), 2740-54.

Di Domenico, F., Perluigi, M., Butterfield, D. A., Cornelius, C., & Calabrese, V. (2010). Oxidative damage in rat brain during aging: interplay between energy and metabolic key target proteins. *Neurochemical Research*. 35(12), 2184-2192.

Eisenhaber, B., Schneider, G., Wildpaner, M., Eisenhaber, F. (2004). A sensitive predictor for potential GPI lipid modification sites in fungal protein sequences and its application to genome-wide studies for *Aspergillus nidulans*, *Candida albicans, Neurospora crassa, Saccharomyces cerevisiae* and *Schizosaccharomyces pombe*. *J Mol Biol.* 337, 243-253.

Frandsen, R. J., Andersson, J. A., Kristensen, M. B., & Giese, H. (2008). Efficient four fragment cloning for the construction of vectors for targeted gene replacement in filamentous fungi. *BMC molecular biology*. 9(1), 70.

Gale, L. R., Bryant, J. D., Calvo, S., Giese, H., Katan, T., O'Donnell, K., ... &

Kistler, H. C. (2005).Chromosome complement of the fungal plant pathogen Fusarium graminearum based on genetic and physical mapping and cytological observations. *Genetics*. 171(3), 985-1001.

Gardiner, D. M., Kazan, K., & Manners, J. M. (2009). Nutrient profiling reveals potent inducers of trichothecene biosynthesis in *Fusarium graminearum*. *Fungal Genetics and Biology*. 46(8), 604-613.

Garrett, T. P., McKern, N. M., Lou, M., Frenkel, M. J., Bentley, J. D., Lovrecz, G. O., ... & Ward, C. W. (1998). Crystal structure of the first three domains of the type-1 insulin-like growth factor receptor. *Nature*. *394*(6691), 395-399.

Ghezzi, P., Bonetto, V., & Fratelli, M. (2005). Thiol-disulfide balance: from the concept of oxidative stress to that of redox regulation. *Antioxidants & Redox Signaling*, 7(7-8), 964-972.

Ghezzi, P., & Bonetto, V. (2003). Redox proteomics: identification of oxidatively modified proteins. *Proteomics*. *3*(7), 1145-1153.

Giese, H., Sondergaard, T.E. and Sorensen, J.L. (2013). The AreA transcription factor in Fusarium graminearum regulates the use of some non-preferred nitrogen sources and secondary metabolite production. *Fungal Biology*. 117, 814–821.

Goswami, R. S., & Kistler, H. C. (2004). Heading for disaster: *Fusarium graminearum* on cereal crops. *Molecular Plant Pathology*. *5*(6), 515-525.

Gruber, C. W., Čemažar, M., Heras, B., Martin, J. L., & Craik, D. J. (2006). Protein disulfide isomerase: the structure of oxidative folding. *Trends in biochemical sciences*. *31*(8), 455-464.

Gulshan, K., Rovinsky, S. A., Coleman, S. T., & Moye-Rowley, W. S. (2005). Oxidant-specific folding of Yap1p regulates both transcriptional activation and nuclear localization. *Journal of Biological Chemistry*. 280(49), 40524-40533.

Gunnaiah, R., Kushalappa, A. C., Duggavathi, R., Fox, S., & Somers, D. J. (2012). Integrated metabolo-proteomic approach to decipher the mechanisms by which wheat QTL (Fhb1) contributes to resistance against *Fusarium graminearum*. *PloS one*. 7(7), e40695.

Guo, B., Styles, C.A., Feng, Q., Fink, G.R. (2000). A *Saccharomyces* gene family involved in invasive growth, cell-cell adhesion, and mating. *Proc Natl Acad Sci USA*. 97, 12158-12163.

Guttman, D. S., McHardy, A. C., & Schulze-Lefert, P. (2014). Microbial genome-enabled insights into plant-microorganism interactions. *Nature Reviews Genetics*. 15(12), 797-813.

Han, Y. K., Kim, M. D., Lee, S. H., Yun, S. H., & Lee, Y. W. (2007). A novel F-box protein involved in sexual development and pathogenesis in *Gibberella zeae*. *Molecular Microbiology*. 63(3), 768-779.

Heller, J., & Tudzynski, P. (2011). Reactive oxygen species in phytopathogenic fungi: signaling, development, and disease. *Annual Review of phytopathology*. 49, 369-390.

Hou, Z., Xue, C., Peng, Y., Katan, T., Kistler, H. C., & Xu, J. R. (2002). A mitogen-activated protein kinase gene (MGV1) in *Fusarium graminearum* is required for female fertility, heterokaryon formation, and plant infection. *Molecular Plant-Microbe Interactions*. 15(11), 1119-1127.

Hou, R., Jiang, C., Zheng, Q., Wang, C., & Xu, J. R. (2015). The AreA transcription factor mediates the regulation of DON synthesis by ammonium and cAMP signaling in Fusarium graminearum. *Molecular Plant Pathology*. DOI: 10.1111/mpp.12254

Jansen, C., Von Wettstein, D., Schäfer, W., Kogel, K. H., Felk, A., & Maier, F. J. (2005). Infection patterns in barley and wheat spikes inoculated with wild-type and trichodiene synthase gene disrupted *Fusarium graminearum*. *Proceedings of the National Academy of Sciences of the United States of America*. 102(46), 16892-16897.

Ji, X. L., Yan, M., Yang, Z. D., Li, A. F., & Kong, L. R. (2013). Shotgun Analysis of the Secretome of *Fusarium graminearum*. *Indian Journal of Microbiology*. 53(4), 400-409.

Jia, L. J., & Tang, W. H. (2015). The omics era of *Fusarium graminearum*: opportunities and challenges. *New Phytologist*, 207(1), 1-3.

Jo, I., Chung, I. Y., Bae, H. W., Kim, J. S., Song, S., Cho, Y. H., & Ha, N. C. (2015). Structural details of the OxyR peroxide-sensing mechanism. *Proceedings of the National Academy of Sciences*. 112(20), 6443-6448.

Joshi, M. (2011). Comparative redox proteomics to investigate role of Nox mediated redox signaling in *Fusarium graminearum* pathogenesis (Masters thesis, University of Manitoba).

Kang, Z., Zingen-Sell, I., & Buchenauer, H. (2005). Infection of wheat spikes by Fusarium avenaceum and alterations of cell wall components in the infected tissue. *European Journal of Plant Pathology*. 111(1), 19-28.

Kawahara, T., Quinn, M. T., & Lambeth, J. D. (2007). Molecular evolution of the

reactive oxygen-generating NADPH oxidase (NOX/Duox) family of enzymes. *BMC evolutionary biology*. 7(1), 109.

Kazan, K., Gardiner, D. M., & Manners, J. M. (2012). On the trail of a cereal killer: recent advances in *Fusarium graminearum* pathogenomics and host resistance. *Molecular Plant Pathology*. 13(4), 399-413.

Kim, H., & Woloshuk, C. P. (2008). Role of AREA, a regulator of nitrogen metabolism, during colonization of maize kernels and fumonisin biosynthesis in Fusarium verticillioides. *Fungal Genetics and Biology*. 45(6), 947-953.

Kim, J. E., Lee, H. J., Lee, J., Kim, K. W., Yun, S. H., Shim, W. B., & Lee, Y. W. (2009). *Gibberella zeae* chitin synthase genes, GzCHS5 and GzCHS7, are required for hyphal growth, perithecia formation, and pathogenicity. *Current Genetics*. 55(4), 449-459.

Kimura, M., Tokai, T., O'Donnell, K., Ward, T. J., Fujimura, M., Hamamoto, H., ... & Yamaguchi, I. (2003). The trichothecene biosynthesis gene cluster of *Fusarium graminearum* F15 contains a limited number of essential pathway genes and expressed non-essential genes. *FEBS Letters*. 539(1), 105-110.

Kimura, M., Tokai, T., Takahashi-Ando, N., Ohsato, S. and Fujimura, M. (2007). Molecular and genetic studies of fusarium trichothecene biosynthesis: pathways,genes, and evolution.*Biosci. Biotechnol. Biochem*. 71, 2105–2123.

Kushalappa, A. C., Kumaraswamy, K. G., Bollina, V., Raghavendra, G., Dion, Y., Rioux, S., ... & Fox, S. (2010). Comprehensive metabolomics and proteomics for fusarium head blight resistance gene discovery and function in *Triticeae*. In *2010 National Fusarium Head Blight Forum* . Milwaukee, WI, USA*,* 20–4.

Kuge, S., Jones, N., & Nomoto, A. (1997). Regulation of yAP-1 nuclear localization in response to oxidative stress. *The EMBO Journal*. 16(7), 1710-1720.

Kwon, S. J., Cho, S. Y., Lee, K. M., Yu, J., Son, M., & Kim, K. H. (2009). Proteomic analysis of fungal host factors differentially expressed by *Fusarium graminearum* infected with *Fusarium graminearum* virus DK21. *Virus Research*. 144(1), 96-106.

Lacaze, I., Lalucque, H., Siegmund, U., Silar, P., & Brun, S. (2015). Identification of NOXD/Pro41 as the homologue of the p22phox NADPH oxidase subunit in fungi. *Molecular microbiology*. 95(6), 1006-1024.

Lara-Ortíz, T., Riveros-Rosas, H., & Aguirre, J. (2003). Reactive oxygen species generated by microbial NADPH oxidase NOXA regulate sexual development in *Aspergillus nidulans*. *Molecular Microbiology*. 50(4), 1241-1255.

Larson, T. M., Kendra, D. F., Busman, M., & Brown, D. W. (2011). *Fusarium verticillioides* chitin synthases CHS5 and CHS7 are required for normal growth and pathogenicity. *Current Genetics*. 57(3), 177-189.

Lee, J., Jurgenson, J. E., Leslie, J. F., & Bowden, R. L. (2008). Alignment of genetic and physical maps of *Gibberella zeae*. *Applied and Environmental Microbiology*. 74(8), 2349-2359.

Lee, S. H., Lee, S., Choi, D., Lee, Y. W., & Yun, S. H. (2006). Identification of the down-regulated genes in a mat1-2-deleted strain of *Gibberella zeae*, using cDNA subtraction and microarray analysis. *Fungal Genetics and Biology*. 43(4), 295-310.

Lee, S. H., Han, Y. K., Yun, S. H., & Lee, Y. W. (2009). Roles of the glyoxylate and methylcitrate cycles in sexual development and virulence in the cereal pathogen *Gibberella zeae*. *Eukaryotic Cell*. 8(8), 1155-1164.

Le Moan, N., Tacnet, F., & Toledano, M. B. (2009). Protein-thiol oxidation, from single proteins to proteome-wide analyses. *Redox-Mediated Signal Transduction*. 175-192.

Leslie, J. F., & Summerell, B. A. (2006). The *Fusarium* laboratory manual (Vol. 2, No. 10). Ames, IA, USA: Blackwell Pub..

Liu, X., Xu, J., Wang, J., Ji, F., Yin, X., & Shi, J. (2015). Involvement of threonine deaminase FgIlv1 in isoleucine biosynthesis and full virulence in *Fusarium graminearum*. *Current genetics*. 61(1), 55-65.

Lombardi, L. M., & Brody, S. (2005). Circadian rhythms in *Neurospora crassa* Clock gene homologues in fungi. *Fungal Genetics and Biology*. 42(11), 887-892.

Lysenko, A., Urban, M., Bennett, L., Tsoka, S., Janowska-Sejda, E., Rawlings, C. *et al*. (2013). Network-based data integration for selecting candidate virulence associated proteins in the cereal infecting fungus *Fusarium graminearum*. *PloS one*. 8(7), e67926.

Lysøe, E., Seong, K-Y., Kistler, H.C. (2011). The transcriptome of *Fusarium graminearum* during the infection of wheat. *Mol Plant Microbe Interact*. 24, 995–1000.

McCormick, S. P., & Alexander, N. J. (2002). *Fusarium* Tri8 encodes a trichothecene C-3 esterase. *Applied and Environmental Microbiology*. 68(6), 2959-2964.

McDonagh, B., Ogueta, S., Lasarte, G., Padilla, C. A., & Bárcena, J. A. (2009). Shotgun

redox proteomics identifies specifically modified cysteines in key metabolic enzymes under oxidative stress in Saccharomyces cerevisiae. *Journal of Proteomics*. 72(4), 677-689.

Ma, L. J., Geiser, D. M., Proctor, R. H., Rooney, A. P., O'Donnell, K., Trail, F., ... & Kazan, K. (2013). *Fusarium* pathogenomics. *Annual Review of Microbiology*. 67, 399-416.

Madeo, F., Herker, E., Maldener, C., Wissing, S., Lächelt, S., Herlan, M., ... & Fröhlich, K. U. (2002). A caspase-related protease regulates apoptosis in yeast. *Molecular Cell*. 9(4), 911-917.

Malagnac, F., Lalucque, H., Lepère, G., & Silar, P. (2004). Two NADPH oxidase isoforms are required for sexual reproduction and ascospore germination in the filamentous fungus *Podospora anserina*. *Fungal Genetics and Biology*. 41(11), 982-997.

Martinez-Lopez, R., Monteoliva, L., Diez-Orejas, R., Nombela, C., & Gil, C. (2004). The GPI-anchored protein CaEcm33p is required for cell wall integrity, morphogenesis and virulence in *Candida albicans*. *Microbiology*. 150(10), 3341-3354.

Martínez-Ruiz, A., & Lamas, S. (2004). S-nitrosylation: a potential new paradigm in signal transduction. *Cardiovascular Research*. 62(1), 43-52.

Markham, P., & Collinge, A. J. (1987). Woronin bodies of filamentous fungi. *FEMS Microbiology Letters*. 46(1), 1-11.

Merhej, J., Boutigny, A.L., Pinson-Gadais, L., Richard-Forget, F., Barreau, C. (2010). Acidic pH as a determinant of TRI gene expression and trichothecene B biosynthesis in *Fusarium graminearum. Chem Anal Control Expo Risk Assess.* 27, 7–717.

Merhej, J., Richard-Forget, F., & Barreau, C. (2011). The pH regulatory factor Pac1 regulates Tri gene expression and trichothecene production in *Fusarium graminearum*. *Fungal Genetics and Biology*. 48(3), 275-284.

Merhej, J., Urban, M., Dufresne, M., Hammond-Kosack, K. E., Richard-Forget, F., & Barreau, C. (2012). The velvet gene, FgVe1, affects fungal development and positively regulates trichothecene biosynthesis and pathogenicity in *Fusarium graminearum*. *Molecular Plant Pathology*. 13(4), 363-374.

Mesterházy, Á. (1995). Types and components of resistance to Fusarium head blight of wheat. *Plant Breed.* 114, 377–386.

Miguel-Rojas, C., & Hera, C. (2015). The F-box protein Fbp1 functions in the invasive

growth and cell wall integrity mitogen-activated protein kinase (MAPK) pathways in *Fusarium oxysporum*. *Molecular Plant Pathology*. doi: 10.1111/mpp.12259

Miller, J.D., Young, J.C., & Sampson, D.R. (1985). Deoxynivalenol and Fusarium head blight resistance in spring cereals. *Phytopathol.* 113, 359–367.

Min, K., Shin, Y., Son, H., Lee, J., Kim, J. C., Choi, G. J., & Lee, Y. W. (2012). Functional analyses of the nitrogen regulatory gene areA in *Gibberella zeae*. *FEMS Microbiology Letters*. 334(1), 66-73.

Min, K., Son, H., Lee, J., Choi, G. J., Kim, J. C., & Lee, Y. W. (2012a). Peroxisome function is required for virulence and survival of *Fusarium graminearum*. *Molecular Plant-Microbe Interactions*. 25(12), 1617-1627.

Miyashita, H., Kuroki, Y., & Matsushima, N. (2014a). Novel leucine rich repeat domains in proteins from unicellular eukaryotes and bacteria. *Protein and Peptide Letters*. 21(3), 292-305.

Miyashita, H., Kretsinger, R. H., & Matsushima, N. (2014b). Comparative Structural Analysis of the Extracellular Regions of the Insulin and Epidermal Growth Factor Receptors whose L1 and L2 Domains have Non-Canonical, Leucine rich Repeats. *Enliven: Bioinform*. 1(1), 005.

Montibus, M., Pinson-Gadais, L., Richard-Forget, F., Barreau, C., & Ponts, N. (2013). Coupling of transcriptional response to oxidative stress and secondary metabolism regulation in filamentous fungi. *Critical Reviews in Microbiology*. 41(3), 295-308.

Mouyna, I., Fontaine, T., Vai, M., Monod, M., Fonzi, W.A. *et al*. (2000).Glycosylphosphatidylinositol-anchored glucanosyltransferases play an active role in the biosynthesis of the fungal cell wall. *J Biol Chem.* 275, 14882-14889. .

Nasmith, C. G., Walkowiak, S., Wang, L., Leung, W. W., Gong, Y., Johnston, A., ... & Subramaniam, R. (2011). Tri6 is a global transcription regulator in the phytopathogen *Fusarium graminearum*. *PLoS Pathog*. 7(9), e1002266.

Nielsen,H., Jacob Engelbrecht, Søren Brunak and Gunnar von Heijne. (1997). .Identification of prokaryotic and eukaryotic signal peptides and prediction of their cleavage sites. *Protein Engineering*, 10:1-6.

Paper, J. M., Scott-Craig, J. S., Adhikari, N. D., Cuomo, C. A., & Walton, J. D. (2007). Comparative proteomics of extracellular proteins in vitro and in planta from the pathogenic fungus *Fusarium graminearum*. *Proteomics*. 7(17), 3171-3183.

Pardo, M., Monteoliva, L., Vázquez, P., Martínez, R., Molero, G., Nombela, C., & Gil, C. (2004). PST1 and ECM33 encode two yeast cell surface GPI proteins important for cell wall integrity. *Microbiology*. 150(12), 4157-4170.

Peñalva, M. A., Tilburn, J., Bignell, E., & Arst, H. N. (2008). Ambient pH gene regulation in fungi: making connections. *Trends in Microbiology*. 16(6), 291-300.

Petersen, T. N., Brunak, S., von Heijne, G., & Nielsen, H. (2011). SignalP 4.0: discriminating signal peptides from transmembrane regions. *Nature methods*. 8(10), 785-786.

Phalip, V., Delalande, F., Carapito, C., Goubet, F., Hatsch, D., Leize-Wagner, E., *et al*. (2005). Diversity of the exoproteome of *Fusarium graminearum* grown on plant cell wall. *Current genetics*. 48(6), 366-379.

Pinton, P., & Oswald, I. P. (2014). Effect of deoxynivalenol and other Type B trichothecenes on the intestine: A review. *Toxins*. 6(5), 1615-1643.

Ponts, N., Pinson-Gadais, L., Barreau, C., Richard-Forget, F., & Ouellet, T. (2007). Exogenous H 2 O 2 and catalase treatments interfere with Tri genes expression in liquid cultures of *Fusarium graminearum*. *FEBS Letters*. 581(3), 443-447.

Popolo, L., Vai, M., Gatti, E., Porello, S., Bonfante, P., Balestrini, R., and Alberghina, L. (1993). Physiological analysis of mutants indicates involvement of the *Saccharomyces cerevisiae* GPI-anchored protein gp115 in morphogenesis and cell separation. *J. Bacteriol*. 175, 1879-1885.

Pritsch, C., Muehlbauer, G. J., Bushnell, W. R., Somers, D. A., & Vance, C. P. (2000). Fungal development and induction of defense response genes during early infection of wheat spikes by *Fusarium graminearum*. *Molecular Plant-Microbe Interactions*. 13(2), 159-169.

Proctor, R. H., Hohn, T. M., & McCormick, S. P. (1995). Reduced virulence of *Gibberella zeae* caused by disruption of a trichthecine toxin biosynthetic gene. *Molecular Plant Microbe Interactions*. 8(4), 593-601.

Rampitsch, C., Subramaniam, R., Djuric-Ciganovic, S., & Bykova, N. V. (2010). The phosphoproteome of *Fusarium graminearum* at the onset of nitrogen starvation. *Proteomics*. 10(1), 124-140.

Rampitsch, C., Leung, W., Blackwell, B., & Subramaniam, R. (2011). Map kinase MGV1: a potential shared control point of butenolide and deoxynivalenol biosynthesis in *Fusarium graminearum*. *Plant Breeding and Seed Science*. 64, 81-88.

Rampitsch, C., Day, J., Subramaniam, R., & Walkowiak, S. (2013). Comparative

secretome analysis of *Fusarium graminearum* and two of its non-pathogenic mutants upon deoxynivalenol induction in vitro. *Proteomics*. 13(12-13), 1913-1921.

Ram, A. F., & Klis, F. M. (2006). Identification of fungal cell wall mutants using susceptibility assays based on Calcofluor white and Congo red. *Nature protocols*. 1(5), 2253-2256.

Reczek, C. R., & Chandel, N. S. (2015). ROS-dependent signal transduction. *Current Opinion in Cell Biology*. 33, 8-13.

Rinnerthaler, M, *et al*. (2012). Yno1p/Aim14p, a NADPH-oxidase ortholog, controls extramitochondrial reactive oxygen species generation, apoptosis, and actin cable formation in yeast. *Proc Natl Acad Sci U S A*. 109(22), 8658-63

Rittenour, W. R., & Harris, S. D. (2013). Glycosylphosphatidylinositol-Anchored Proteins in *Fusarium graminearum*: Inventory, Variability, and Virulence. *PLoS ONE*. 8(11).

Roncero, C., & Duran, A. (1985). Effect of Calcofluor white and Congo red on fungal cell wall morphogenesis: in vivo activation of chitin polymerization. *Journal of Bacteriology*, *163*(3), 1180-1185.

Ruepp, A., Zollner, A., Maier, D., Albermann, K., Hani, J., Mokrejs, M., ... & Mewes, H. W. (2004). The FunCat, a functional annotation scheme for systematic classification of proteins from whole genomes. *Nucleic Acids Research*. 32(18), 5539-5545.

Rudd, J. C., Horsley, R. D., McKendry, A. L., & Elias, E. M. (2001). Host plant resistance genes for *Fusarium head blight*. *Crop Science*. 41(3), 620-627.

Schmiedel, J., Blaukat, A., Li, S., Knöchel, T., & Ferguson, K. M. (2008). Matuzumab binding to EGFR prevents the conformational rearrangement required for dimerization. *Cancer cell*. 13(4), 365-373.

Segmüller, N., Kokkelink, L., Giesbert, S., Odinius, D., van Kan, J., & Tudzynski, P. (2008). NADPH oxidases are involved in differentiation and pathogenicity in *Botrytis cinerea*. *Molecular Plant-Microbe Interactions*. 21(6), 808-819.

Sela-Buurlage, M. B., Ponstein, A. S., Bres-Vloemans, S. A., Melchers, L. S., van den Elzen, P. J., & Cornelissen, B. J. (1993). Only specific tobacco (*Nicotiana tabacum*) chitinases and [beta]-1, 3-glucanases exhibit antifungal activity. *Plant Physiology*. 101(3), 857-863.

Seong, K. Y., Pasquali, M., Zhou, X., Song, J., Hilburn, K., McCormick, S., ... & Kistler,

H. C. (2009). Global gene regulation by *Fusarium* transcription factors Tri6 and Tri10 reveals adaptations for toxin biosynthesis. *Molecular Microbiology*. 72(2), 354-367.

Shenton, D., & Grant, C. (2003). Protein S-thiolation targets glycolysis and protein synthesis in response to oxidative stress in the yeast *Saccharomyces cerevisiae*. *Biochem. J*. 374, 513-519.

Soanes, D. M., & Talbot, N. J. (2010). Comparative genome analysis reveals an absence of leucine-rich repeat pattern-recognition receptor proteins in the kingdom fungi. *PLoS One*. 5(9), e12725.

Son, H., Min, K., Lee, J., Choi, G. J., Kim, J. C., & Lee, Y. W. (2012). Differential roles of pyruvate decarboxylase in aerial and embedded mycelia of the ascomycete *Gibberella zeae*. *FEMS Microbiology Letters*. 329(2), 123-130.

Son, M., Lee, K. M., Yu, J., Kang, M., Park, J. M., Kwon, S. J., & Kim, K. H. (2013). The HEX1 gene of *Fusarium graminearum* is required for fungal asexual reproduction and pathogenesis and for efficient viral RNA accumulation of *Fusarium graminearum virus 1*. *Journal of virology*. 87(18), 10356-10367.

Takemoto, D., Tanaka, A., & Scott, B. (2007). NADPH oxidases in fungi: diverse roles of reactive oxygen species in fungal cellular differentiation. *Fungal Genetics and Biology*. 44(11), 1065-1076.

Taylor, R. D., Saparno, A., Blackwell, B., Anoop, V., Gleddie, S., Tinker, N. A., & Harris, L. J. (2008). Proteomic analyses of *Fusarium graminearum* grown under mycotoxin-inducing conditions. *Proteomics*, *8*(11), 2256-2265.

Trail, F. (2009). For blighted waves of grain: *Fusarium graminearum* in the postgenomics era. *Plant Physiology*. 149(1), 103-110.

Tudzynski, P., Heller, J., & Siegmund, U. (2012). Reactive oxygen species generation in fungal development and pathogenesis. *Current opinion in microbiology*. 15(6), 653-659.

Urban, M., Mott, E., Farley, T., & Hammond-Kosack, K. (2003). *The Fusarium graminearum* MAP1 gene is essential for pathogenicity and development of perithecia. *Molecular Plant Pathology*. 4(5), 347-359.

Vishwakarma, R.A., & Menon, A.K. (2005). Flip-flop of glycosylphosphatidylinositols (GPIs) across the endoplasmic reticulum. *Chem Commun.* 4, 453-455.

Walkowiak, S., Bonner, C. T., Wang, L., Blackwell, B., Rowland, O., & Subramaniam,

R. (2015). Intraspecies interaction of *Fusarium graminearum* contributes to reduced toxin production and virulence. *Molecular Plant-Microbe Interactions*, http://dx.doi.org/10.1094/MPMI-06-15-0120-R

Wang, L., Mogg, C., Walkowiak, S., Joshi, M., & Subramaniam, R. (2014). Characterization of NADPH oxidase genes NOXA and NOXB in *Fusarium graminearum*. *Canadian Journal of Plant Pathology*, *36*(1), 12-21.

Ward, C. W., & Garrett, T. P. (2001). The relationship between the L1 and L2 domains of the insulin and epidermal growth factor receptors and leucine-rich repeat modules. *BMC bioinformatics*. 2(1), 4

Wegulo, S. N., Baenziger, P. S., Nopsa, J. H., Bockus, W. W., & Hallen-Adams, H. (2015). Management of Fusarium head blight of wheat and barley. *Crop Protection*. 73, 100-107.

Wiedman, J. M., Fabre, A. L., Taron, B. W., Taron, C. H., & Orlean, P. (2007). In vivo characterization of the GPI assembly defect in yeast mcd4-174 mutants and bypass of the Mcd4p-dependent step in mcd4Δ cells. *FEMS yeast research*. 7(1), 78-83.

Woloshuk, C. P., & Shim, W. B. (2013). Aflatoxins, fumonisins, and trichothecenes: a convergence of knowledge. *FEMS microbiology reviews*. 37(1), 94-109.

Yang, F. E. N., Jensen, J. D., Svensson, B., Jørgensen, H. J., Collinge, D. B., & Finnie, C. (2012). Secretomics identifies *Fusarium graminearum* proteins involved in the interaction with barley and wheat. *Molecular Plant Pathology*. 13(5), 445-453.

Yang, F., Finnie, C., & Jacobsen, S. (2011). Application of proteomics to investigate barley-*Fusarium graminearum* interaction. *Enzyme and Protein*. (Master's thesis). Retrieved from, http://orbit.dtu.dk/fedora/objects/orbit:89410/datastreams/file_6327491/content

Yates, J. R., Ruse, C. I., & Nakorchevsky, A. (2009). Proteomics by mass spectrometry: approaches, advances, and applications. *Annual Review of Biomedical Engineering*. 11, 49-79.

Zheng, M., Åslund, F., & Storz, G. (1998). Activation of the OxyR transcription factor by reversible disulfide bond formation. *Science*. 279(5357), 1718-1722.

Zhang, L., Li, B., Zhang, Y., Jia, X., & Zhou, M. (2015). Hexokinase plays a critical role in deoxynivalenol (DON) production and fungal development in *Fusarium graminearum*. *Molecular Plant Pathology*. DOI: 10.1111/mpp.12258

Zhu, H., Nowrousian, M., Kupfer, D., Colot, H. V., Berrocal-Tito, G., Lai, H.,

Dunlap, J. C., *et al*. (2001). Analysis of expressed sequence tags from two starvation, time-of-day-specific libraries of *Neurospora crassa* reveals novel clock-controlled genes. *Genetics*. 157(3), 1057-1065.